

Санкт-Петербургский политехнический университет Петра
Великого Институт прикладной математики и механики Кафедра
«Гидроаэродинамика, горение и теплообмен»

Курс лекций «Современные методы расчета турбулентных
течений»

(http://cfд.spbstu.ru/agarbaruk/lecture/modern_methods/)

**«Расчет развитого течения в плоском канале с
использованием вихреразрешающих подходов»**

Гарбарук Андрей Викторович (agarbaruk@mail.ru)

Гусева Екатерина Константиновна (katia.guseva@inbox.ru)

2018

Постановка задачи

Задача о периодическом течении в плоском канале рассматривается при числе Рейнольдса $Re_\tau = H/2 \cdot U_\tau / \nu = 395$ (при расчетах необходимо использовать значение числа Рейнольдса прописанное в задании), где H – высота канала, U_τ – динамическая скорость, ν – кинематическая вязкость.

Расчетная область для данной задачи берется равной $4H$ и $1.5H$ в направлении течения (X) и направлении поперек течения соответственно (Z).

Для рассматриваемого числа Рейнольдса расчетная сетка состоит из $81 \times 81 \times 61$ узлов (для других чисел Рейнольдса количество узлов по Y будет отличаться) и строится равномерной в направлении течения и в направлении поперек течения с шагами $\Delta x/H = 0.05$ и $\Delta z/H = 0.025$ соответственно (в переменных закона стенки $\Delta X^+ = 40$, $\Delta Z^+ = 20$). В направлении по нормали к стенке расчетная сетка строится со сгущением с коэффициентом 1.15, при этом параметры сетки в переменных закона стенки составляют $\Delta Y^+ = 0.3 \div 30$ (при построении расчетной сетки для более высоких чисел Рейнольдса необходимо увеличить число узлов по y и следить за тем, чтобы пристенный шаг сетки в переменных закона стенки был всегда меньше 1).

В направлении течения и в направлении поперек течения задаются периодические граничные условия¹, при этом градиент давления $dp/dx = -2 \cdot \rho \cdot u_\tau^2 / H$ задается в определяющих уравнениях при помощи объемного источника в уравнениях баланса импульса. При таком подходе значение среднерасходной скорости определяется из решения и поэтому зависит от выбора подсеточной модели турбулентности. Шаг по времени для данной задачи задается равным $\Delta t = 0.001 \cdot H / u_\tau$, что соответствует числу Куранта меньше единицы во всей расчетной области.

Размерная постановка для некоторых чисел Рейнольдса, а также другие детали постановки могут быть найдены в Приложении 1.

Выбор численной схемы

При решении задачи вихререзающими методами необходимо использовать нестационарную ветвь ANSYS-FLUENT². Следует особо отметить, что точность расчета такими методами зависит от используемого численного метода. Поэтому, основываясь на результатах тестирования (см. Приложение 1 и Приложение 2), рекомендуется использовать следующие настройки вычислительного алгоритма:

- Для интерполяции скорости на грань в конвективных слагаемых рекомендуется использовать центрально разностную схему второго порядка (в обозначениях ANSYS-FLUENT – Central Differencing или CD).
- Для интерполяции давления на грань рекомендуется использовать взвешенную противопоточную схему первого и второго порядка (в обозначениях ANSYS-FLUENT – Standard).

¹ Для задания периодических граничных условий для границ с номерами bndnum1 и bndnum2 необходимо ввести следующую команду в текстовом интерфейсе ANSYS FLUENT:
/mesh/modify-zone/make-periodic bndnum1 bndnum2 n y

² Задачу необходимо решать с использованием кода общего назначения ANSYS FLUENT версии 14 и выше.

- Для вычисления градиентов рекомендуется использовать схему, основанную на теореме Гаусса-Грина (в обозначениях ANSYS-FLUENT – Green Gauss Cell Based или GGCB).
- Для аппроксимации производных по времени рекомендуется использовать двуслойную схему Эйлера второго порядка (в обозначениях ANSYS-FLUENT – Second Order Implicit или SOI).
- Для продвижения по времени рекомендуется использовать итерационный метод SIMPLEC, при этом на каждом шаге по времени необходимо проводить как минимум 10 итераций по псевдо-времени.
- Для обеспечения максимально быстрой сходимости решения на каждом шаге по времени рекомендуется установить все релаксационные параметры равными 1.

Проведение расчета

Расчет периодического течения в плоском канале с использованием ANSYS-FLUENT проводится в два этапа.

Вначале проводится стационарный расчет по модели SST во всей расчетной области. Далее на имеющееся стационарное поле скорости накладываются искусственные турбулентные пульсации³ и полученное поле используется в качестве начального приближения для расчетов на втором этапе. Следует отметить, что после наложения турбулентных пульсаций необходимо удостовериться в том, что полученное поле отличается от первоначального стационарного поля. Кроме того, в случае использования SST DES, SST IDDES, необходимо также проинициализировать величины кинетической энергии турбулентности и удельной диссипации так, чтобы уровень начальной турбулентной вязкости был низким. В противном случае будут использованы поля K и ω , полученные по RANS модели SST, и высокая вязкость приведет к диссипации турбулентных структур, а решение может выйти на стационарный режим. Другим решением данной проблемы может быть проведение предварительного расчета без подсеточной модели или с алгебраической моделью.

На втором этапе проводится нестационарный расчет с использованием того или иного вихреразрешающего подхода в соответствии с расчетным заданием и вышеприведенными указаниями по выбору оптимальных настроек вычислительного алгоритма. Следует отметить, что при проведении расчетов необходимо контролировать изменение среднего значения трения (τ_w) на стенках канала и значения среднерасходной скорости (U_b) во времени. Для этого рекомендуется использовать *surface monitors*. После того, как изменение вышеупомянутых величин во времени оказывается статистически установившимся (среднее значение перестает меняться во времени), необходимо получить осредненные по времени величины. Для этого необходимо сбросить нестационарную статистику для текущего решения⁴ и провести расчет как минимум 5000 шагов по времени со сбором временной статистики (*data sampling for time statistics* в меню *run calculation*).

После окончания осреднения можно преступать к обработке результатов.

³ Для этого необходимо открыть решение по SST модели (cas и dat файлы) и в текстовом интерфейсе ввести следующую команду:

/solve/initialize/init-instantaneous-vel

⁴ Для сброса нестационарной статистики необходимо в текстовом интерфейсе ввести следующую команду:

/solve/initialize/init-flow-statistics

Обработка результатов и требования к отчету

Обработку результатов необходимо проводить в пакетах ANSYS CFD-Post или Tecplot. Для анализа результатов вначале необходимо вычислить осредненное по стенкам канала значение динамической скорости:

$$u_{\tau}=(\tau_{w,MEAN} /\rho)^{0.5}$$

Здесь $\tau_{w,MEAN}$ – значение осредненного по времени трения на стенке, ρ – плотность. Далее основываясь на значении u_{τ} необходимо вычислить и построить следующие характеристики:

$$y^{+}=y \cdot u_{\tau} / \nu$$

$$U^{+}=U_{MEAN} / u_{\tau}$$

$$U'^{+}=U_{RMS} / u_{\tau}$$

$$V'^{+}=V_{RMS} / u_{\tau}$$

$$W'^{+}=W_{RMS} / u_{\tau}$$

$$UV^{+}=-UV / u_{\tau}^2 \text{ (полные напряжения, а также разрешенную и моделируемую части)}$$

$$\langle v_t \rangle / \nu$$

Здесь ν – кинематическая вязкость, $\langle v_t \rangle$ - осредненная турбулентная вязкость.

Для визуализации течения необходимо построить изоповерхность Q-критерия, вычисляемого в виде:

$$Q=|S^2-\Omega^2| \quad \text{Q-критерий}$$

$$S=(2S_{ij}S_{ij})^{0.5} \quad \text{второй инвариант тензора завихренности (завихренность)}$$

$$\Omega=(2\Omega_{ij}\Omega_{ij})^{0.5} \quad \text{второй инвариант тензора скоростей деформации}$$

При визуализации изоповерхности обычно окрашивают той или иной физической величиной (скорость, турбулентная вязкость и т.д.).

Отчет должен содержать в себе введение, включающее в себя цель работы и средства ее решения, определяющие уравнения (см. главу 4 в файле Fluent_Theory.pdf) и методы их решения (см. главу 20 в файле Fluent_Theory.pdf), постановку задачи, результаты расчетов и выводы.

Результаты должны быть представлены в виде, максимально близком к представленному в приложении 1, и должны содержать сравнение результатов расчета с данными DNS для следующих величин: $U^{+}(y^{+})$, $UV^{+}(y)$, $U'^{+}(y)$, $V'^{+}(y)$, $W'^{+}(y)$. При сравнении касательных напряжений с данными DNS следует представить разрешенную и моделируемую части напряжений, а также полные касательные напряжения.

Также в отчете должна содержаться визуализация течения при помощи изоповерхностей Q-критерия и мгновенных поля скорости и завихренности в плоскости XY. Кроме того необходимо представить мгновенное поле отношения турбулентной

вязкости к кинематической (ν_t/ν), а также графики зависимости осредненной (по времени или пространству) величины ν_t/ν от координаты y .

Помимо этого необходимо представить изменение среднерасходной скорости U_b и среднего трения на стенке τ_w во времени.

Для сравнения результатов необходимо использовать данные прямого численного моделирования⁵ (данные можно найти на сайте <http://torroja.dmt.upm.es/channels/data/statistics/>).

Постановка задачи на счет на кластере

При постановке задачи на счет на вычислительном кластере на N ядрах необходимо запустить в командной строке команду вида (более подробно о постановке задачи на кластере можно проконсультироваться на кафедре):

```
fluent 3ddp -tN -i"run.jou" >fluent.txt
```

В файле run.jou необходимо поместить набор скриптовых команд для постановки задачи на счет. Ниже приведен пример такого скрипта (строка начинающаяся символом ; является закомментированной и может быть удалена):

```
;read case and data file with name 'run'  
/rcd "run"  
;initialize time statistics  
/solve/initialize/init-flow-statistics  
;Perform 5000 time-steps with 10 sub-iteration per time-step.  
;NOTE: If you have any monitors in your case you should add the same number of 'y' symbols  
/solve/dual-time-iterate 5000 10 y y y  
;write case and data file with name 'run-05000'  
/wcd "run-05000"  
;exit from FLUENT  
/exit y
```

⁵ S. Hoyas and J. Jimenez, (2008) "Reynolds number effects on the Reynolds-stress budgets in turbulent channels", Phys. Fluids, Vol. 20, 101511.

IDDES of developed channel flow in ANSYS Fluent

M. S. Gritskevich, A. V. Garbaruk, and F. R. Menter

1. Introduction

Most current CFD simulations are based on the Reynolds Averaged Navier Stokes (RANS) equations. This allows the solution of complex flow problems in steady state mode with manageable computing power. However, there are numerous situations where it is not suitable to average out all turbulence content from the simulation for mainly two reasons.

There are many flows where RANS models are not accurate enough to provide the required quality in the simulation:

Flows with large separation zones like flows past bluff bodies.

Strongly swirling flows in combustion chambers.

Largely unguided flows like in HVAC.

Flows where the unsteady turbulence information is required for other models:

Acoustics.

Vortex cavitation.

Some FSI problems.

Unsteady heat loading and related fatigue.

For such situations, at least a portion of the turbulence spectrum has to be resolved in at least a portion of the numerical domain. Such models are generally termed here Scale-Resolving Simulation (SRS). The most widely known such modeling concept is Large Eddy Simulation (LES). It is based on the approach of resolving large turbulent structures in space and time down to the grid limit everywhere in the flow. However, while widely used in the academic community, LES had very limited impact on industrial simulations. The reason lies in the excessively high resolution requirements for wall boundary layers. Near the wall, the largest scales in the turbulent spectrum are nevertheless geometrically very small and require a very fine grid and a small time step. In addition, unlike RANS, the grid cannot only be refined in the wall normal direction, but also needs to resolve turbulence in the wall parallel plane. This can only be achieved for flows at very low Reynolds number and on very small geometric scales (the extent of the LES domain cannot be much larger than 10-100 times the boundary layer thickness parallel to the wall). For this reason the use of LES is only recommended for flows where wall boundary layers are not relevant and need not be resolved or for flows where the boundary layers are laminar due to the low Reynolds number.

However, there are only very few such flows and other approaches need to be employed. A promising approach to overcome the Reynolds number scaling limitations of LES is the approach proposed by Shur (Shur, et al., 2008) in their method termed Improved Delayed Detached Eddy simulation (IDDES). It can be run in standard DDES mode, meaning the wall boundary layer is shielded from the DES limiter to avoid Grid Induced Separation (GIS) (Menter, et al., 2004). However, the IDDES model is also designed to operate in Wall Modeled LES (WMLES) mode.

In this situation, the RANS portion of the model is only activated in the inner part of the logarithmic layer and the outer part of the boundary layer is covered by a modified LES formulation. Since the inner portion of the boundary layer is responsible for the Reynolds number dependency of the LES model, the IDDES approach can be applied on the same grid resolution to an ever increasing Re number for channel flow simulations.

It is to be noted that for wall boundary layers, the Re number scaling is not entirely avoided, as the thickness of the boundary layer declines relative to body dimensions with increasing Re number. Assuming a certain number of grid nodes per 'boundary layer volume', the overall grid spacing will decrease and the overall number of cells will increase with Re number.

In addition to IDDES, a simplified algebraic version is implemented into Fluent. It allows for a more consistent combination with embedded LES, where an algebraic LES model is required in the LES zone.

The IDDES formulation has been implemented into the CFD code ANSYS-Fluent 12 and tested and calibrated for a series of flows.

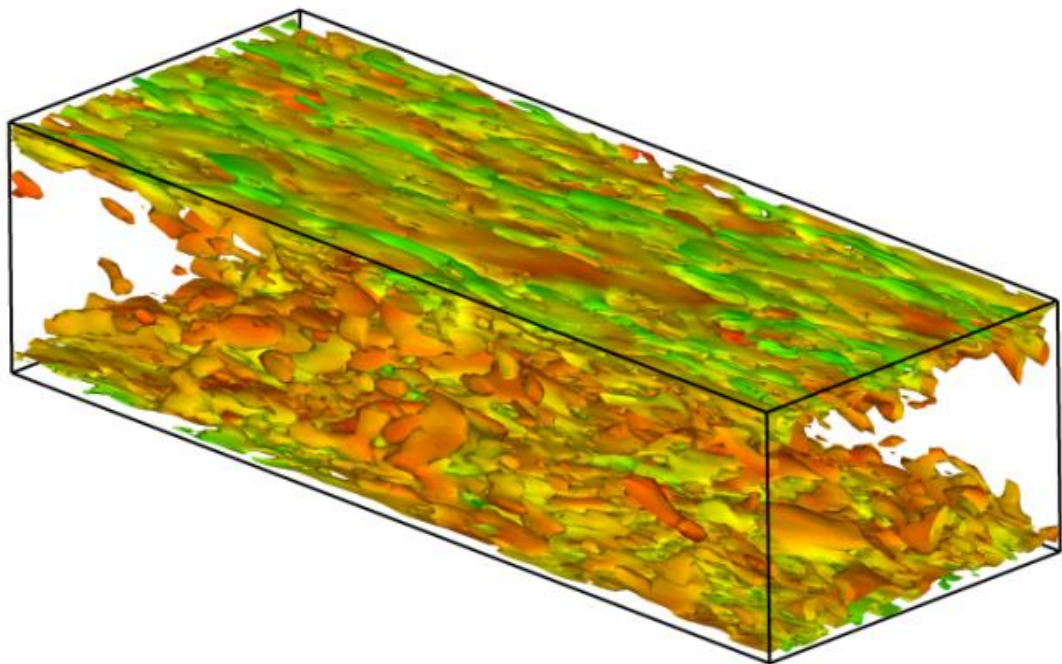
Wall Modeled LES (WMLES)

The final mode of operation is Wall Modeled LES (WMLES). In this mode the RANS model only covers the inner part of the logarithmic wall layer, whereas the rest of the boundary layer is computed in RANS mode. The goal of this formulation is to avoid the Reynolds number sensitivity of wall-resolved LES.

Periodic Channel

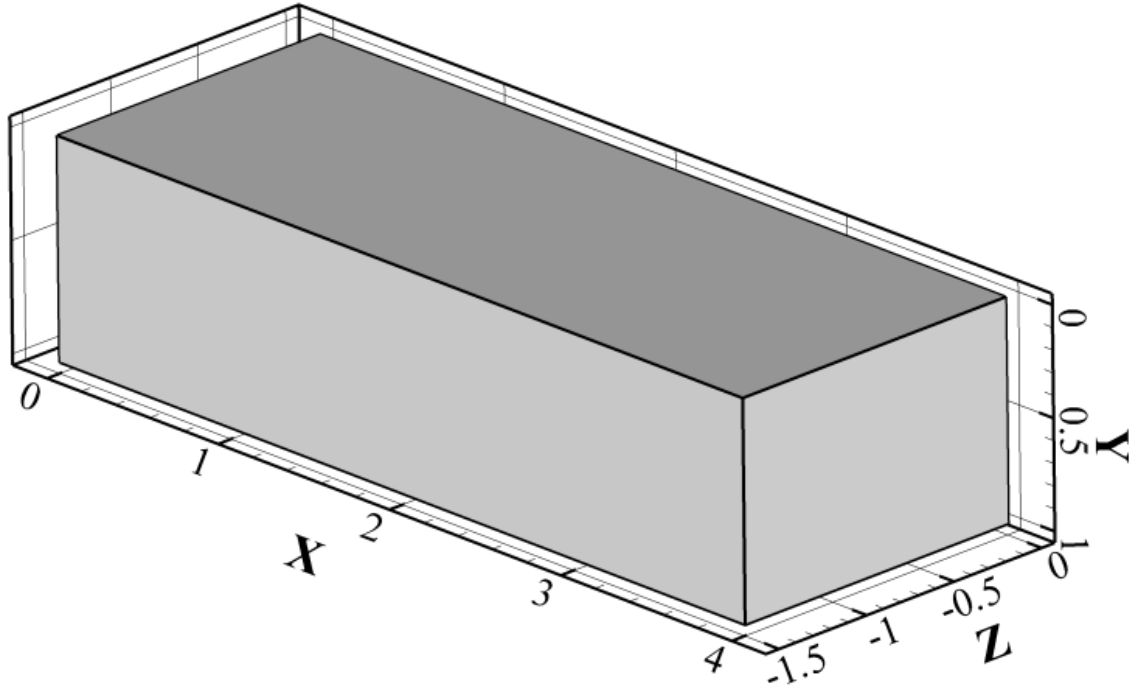
Test Case Description

Periodic Channel is a benchmark test case which is commonly used for turbulence model investigation due to its geometric simplicity (Shur, et al., 2008). For relatively low Reynolds numbers (based on friction velocity) DNS data are available for this test case (Moser, et al., 1999). One important issue, which is especially significant for SRS turbulence models, is that Periodic Channel does not need any unsteady boundary conditions, as unsteadiness is naturally sustained by periodic conditions. That is why no additional assumptions and no additional information are required. An example of such a flow is presented in Fig. 5.1, where isosurfaces of the Q-criterion colored with velocity are plotted.



Isosurface of Q-criterion colored by velocity

A computational domain for this test case is shown in figure 5.2. The characteristic length, which determines the geometry, is a channel height H which was taken equal to 1 [m] in current study. Dimensions of the computational domain in X, Y, and Z directions were taken equal to $4 \cdot H$, H , and $1.5 \cdot H$ respectively.



Computational domain for the Periodic Channel test case

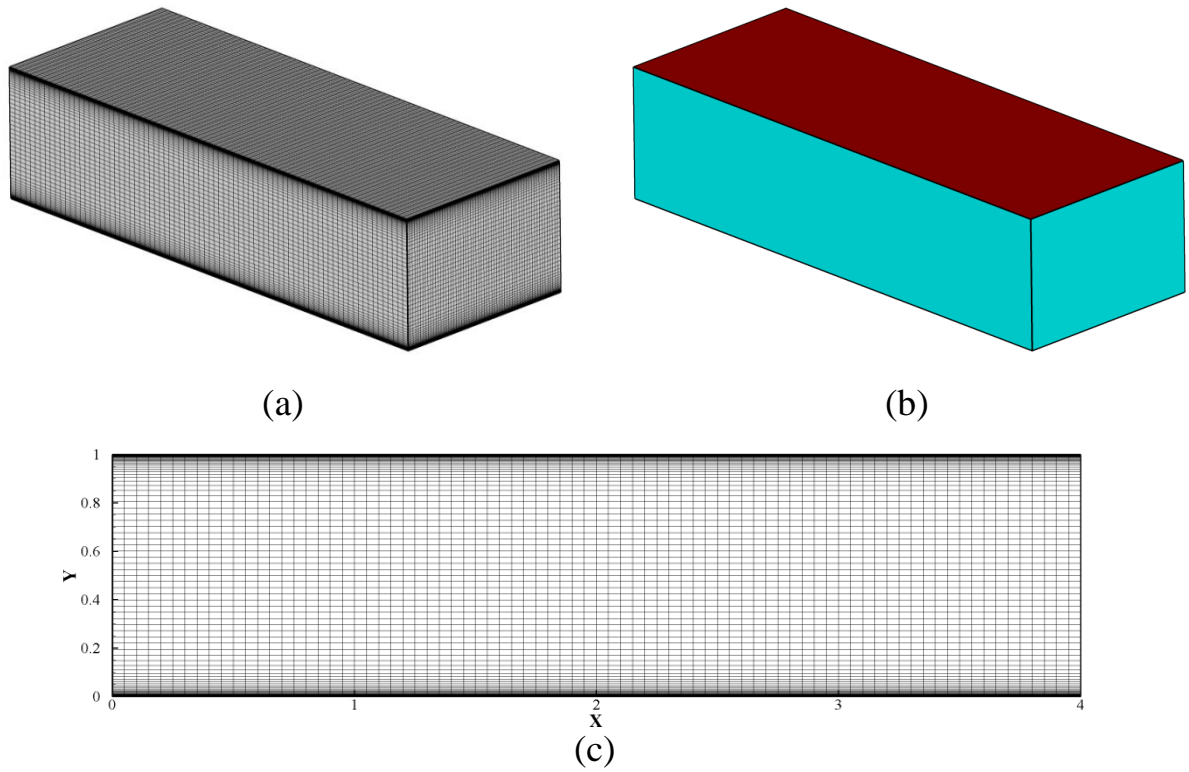
The simulation was performed in transient formulation for incompressible fluid. A summary of physical parameters is presented in table 5.1.

The summary of physical parameters

Re_{τ} [-]	395	760	1100	2400	18000
U_{τ} [$m \cdot s^{-1}$]	1.0	1.0	1.0	1.0	1.0
Δt [s]	0.001	0.001	0.001	0.001	0.001
μ [$Pa \cdot s$]	1.27×10^{-3}	6.58×10^{-4}	4.55×10^{-4}	2.08×10^{-4}	2.78×10^{-5}
ρ [$kg \cdot m^{-3}$]	1.0	1.0	1.0	1.0	1.0
dp/dx [$Pa \cdot m^{-1}$]	-2.0	-2.0	-2.0	-2.0	-2.0

An example of the computational grid used for the test case is shown in Fig 5.3-a, c. The base grid was uniform in X and Z direction with step 0.05 [m] and 0.025 [m] respectively. In wall normal direction the grid was stretched with a factor of 1.15. For all considered test cases, except the investigation of wall function and model interaction, the value of y^+ was set to 0.2, which means that the governing equations are integrated to the wall. The base grid for different Reynolds number has from 380 000 to 624 000 cells. A complete summary of all used grids is presented in table 5.2.

In Fig. 5.3-b all applied boundary conditions are shown. On cyan colored boundaries periodic boundary conditions and on red colored boundaries no-slip wall conditions were applied. The influence of the pressure gradient was taken into account via a source term in the momentum equations.



Developed channel flow computational grid for $Re_\tau = 18000$ (a) and applied boundary conditions (b)

For test cases with $Re_\tau = 395$ and $Re_\tau = 18000$ a refined grid was generated. It was obtained from the coarse grid by multiplying the nodes number in each spatial direction by a factor of 1.5. For the test case with $Re_\tau = 18000$ two high-Reynolds grids were generated with non-dimensional wall normal grid step equal to 8 and 40.

The summary of grids parameters

Re_τ	Grid Name	Cells Number	Nodes Number	ΔX^+	ΔY^+	ΔZ^+
395	Grid 1	384 000	81×81×61	40.0	0.2 ÷ 30	20.0
395	Grid 2	1 764 000	141×141×91	26.6	0.2 ÷ 20	13.3
760	-	480 000	81×101×61	76.9	0.2 ÷ 30	38.5
1100	-	480 000	81×101×61	111.4	0.2 ÷ 30	55.7
2400	-	528 000	81×111×61	243.0	0.2 ÷ 30	121.5
18000	Grid 1	102 900	41×76×31	3645.4	0.2 ÷ 52	1822.7
18000	Grid 2	624 000	81×131×61	1822.7	0.2 ÷ 30	911.4
18000	Grid 3	2 457 000	141×196×91	1215.1	0.2 ÷ 20	607.6
18000	-	384 000	81×81×61	1822.7	8 ÷ 20	911.4
18000	-	288 000	81×61×61	1822.7	40 ÷ 20	911.4

For all considered test cases, the following numerical setup was used. Since an unsteady incompressible flow is considered, a transient pressure based solver with Non-Iterative Time Advancement based on Fractional Time Step method was used. A second order scheme was used for the approximation of time derivatives. A second order central difference scheme was used for the approximation of the convection terms in momentum equations. A first order upwind scheme was used for turbulence equations. The Green-Gauss cell based method was used for interpolation

of variables on faces. A PREssure STaggering Option (PRESTO) was used for pressure interpolation scheme.

For most computational grids the value of y^+ is less than 1. That is why there is no need in any additional assumptions for wall boundary conditions. The Enhanced Wall Treatment was used at no-slip walls. This allows for a switch from integration to the wall on fine grids to a wall function formulation on coarse grids.

Results

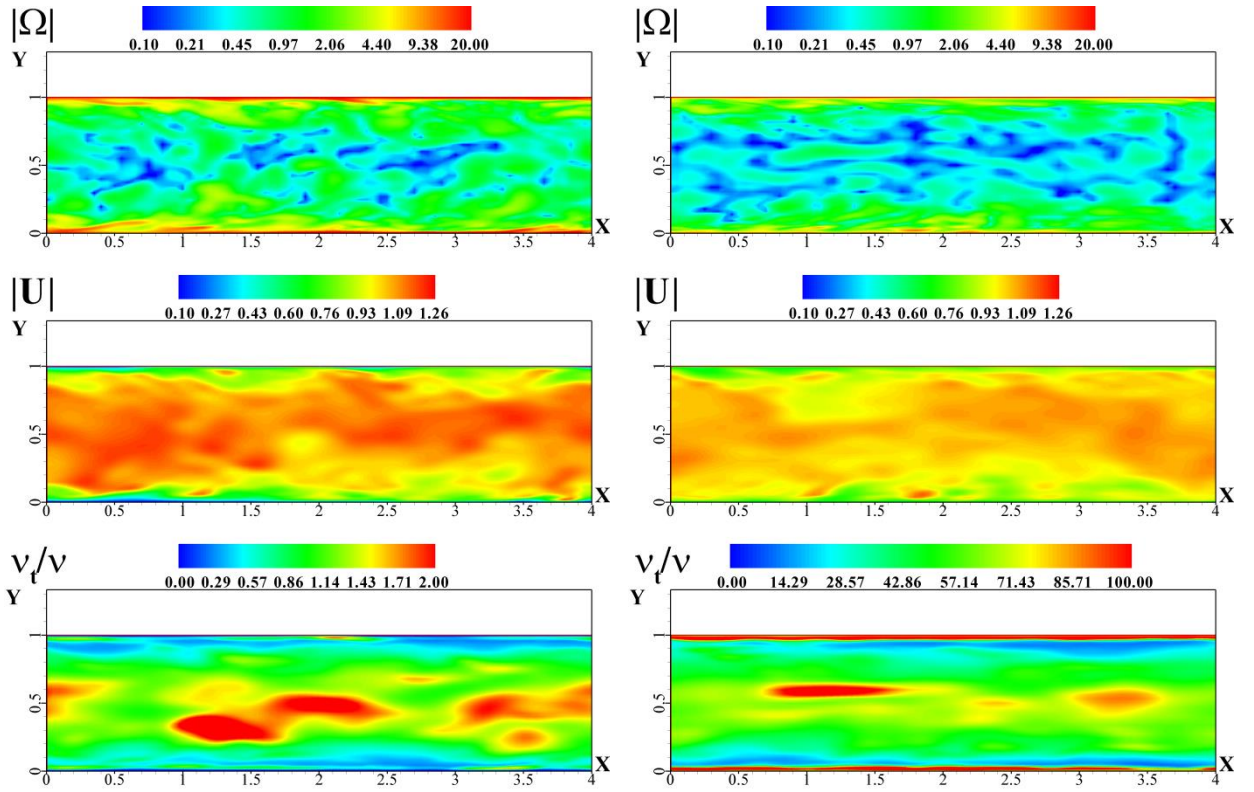
The Periodic Channel test case was investigated with the use of the Algebraic WMLES and the IDDES turbulence model, with different numerics, and with different grids. For verification of the IDDES turbulence model a series of computations with different Reynolds numbers was conducted, and these results were compared with the results obtained with the NTS in-house code (Shur, et al., 2008).

Contours of vorticity, velocity magnitude and eddy viscosity based on instantaneous flow field are presented in figure 5.4.

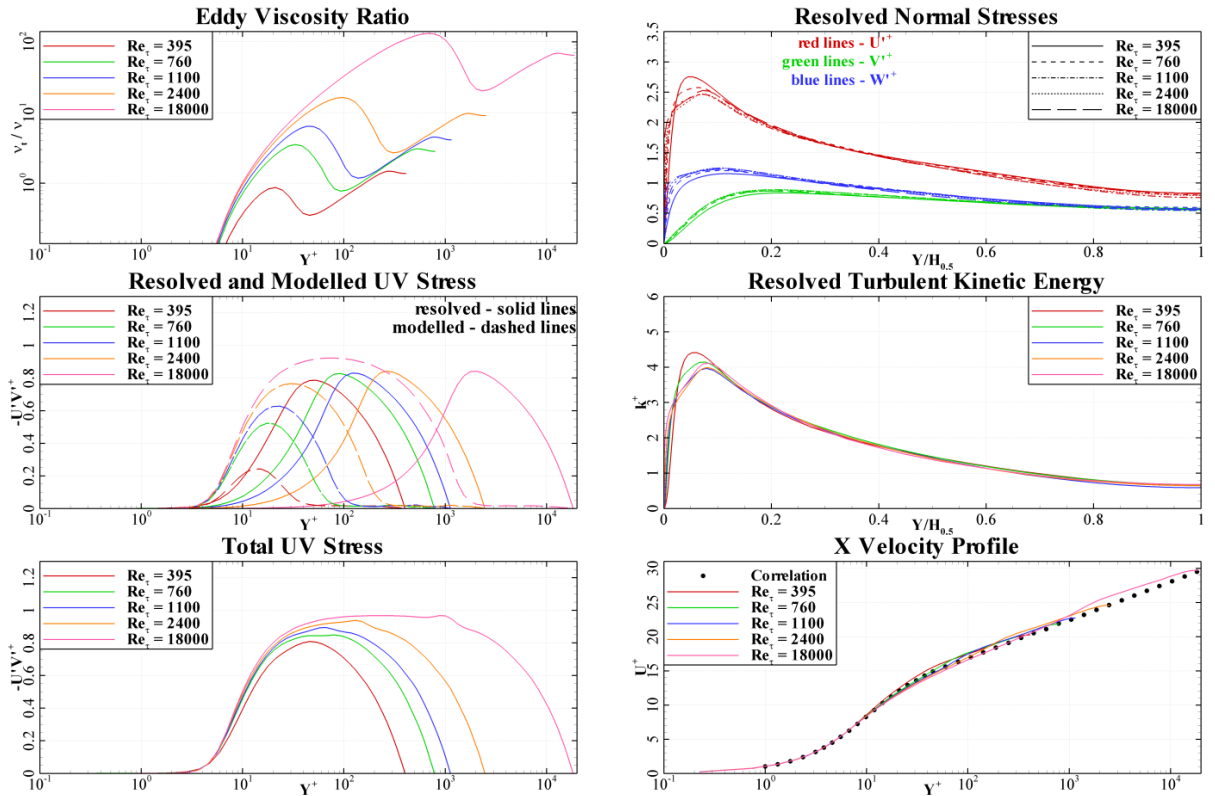
In figures 5.5-5.6 the Reynolds number scaling is presented for IDDES and Algebraic WMLES. As it can be seen, there is a slight log-layer mismatch for both models, but its magnitude is relatively small.

In figures 5.7-5.11 a comparison with the NTS code is presented. As one can see, for all Reynolds numbers, there is a trend of over-prediction of the resolved kinetic energy. For low Reynolds number ($Re_\tau = 395, 760, 1100$) Fluent velocity profile is very close to the NTS code, while for higher Reynolds numbers ($Re_\tau = 2400, 18000$) there is a slightly larger log-layer mismatch with Fluent than with the NTS code. This is a result of differences in numerics. In Fluent a 2nd order central scheme is used, whereas the NTS code employs 4th order central differences. The first test which was done to investigate the model behavior is a grid refinement study. Three grids were considered namely Grid 1, Grid 2, and Grid 3. Grid 2 is a basic grid used for investigation of Reynolds number effects. Grid 3 is obtained by multiplying the nodes number of nodes in every spatial direction with a factor of 1.5, and Grid 1 is obtained by dividing the nodes number in every spatial direction by a factor of 2. The results for this study are presented in figures 5.12 – 5.13. The test was conducted for the highest and lowest Reynolds number. One can see that there is no improvement in log-layer mismatch for $Re_\tau = 18000$ even on finest grid. It also can be seen that the results for Grid 1 are very close to results obtained on Grid 2 and Grid 3.

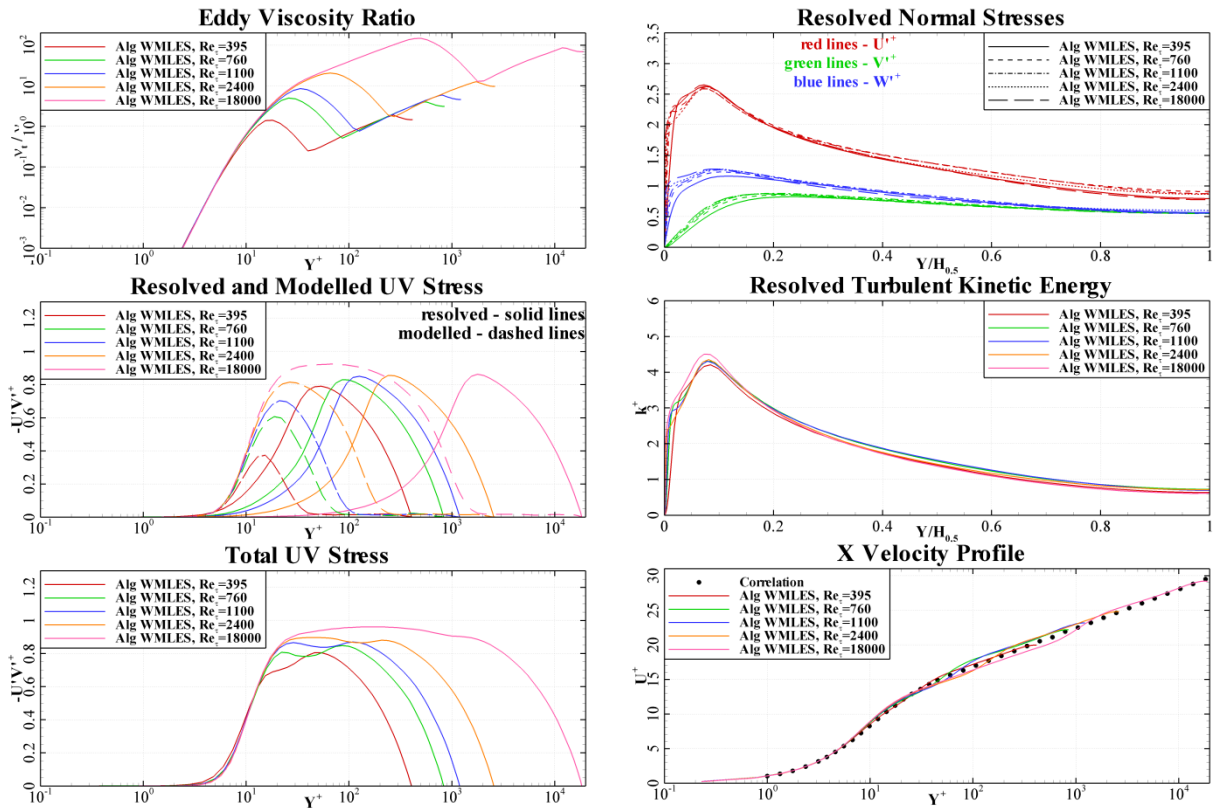
The last test was done to investigate the ability of IDDES to work with automatic and enhanced wall treatment. The test was conducted for $Re_\tau = 18000$. The computations were performed on three grids with y^+ equal to 0.2, 8, and 40. The results of this test are presented in figures 5.14 – 5.15. As one can see, for y^+ equal to 0.2 both wall treatment methods give the same results due to the equations can be integrated up to the wall. For y^+ equal to 8 enhanced wall treatments gives wrong velocity profile in the log-layer, while automatic wall treatment gives absolutely correct profile for both y^+ equal to 8 and 40. One should notice that both methods give very small differences for stresses and eddy viscosity. Concluding the above, it can be stated that IDDES is capable to work with automatic wall treatment and relatively large y^+ without any damage to accuracy.



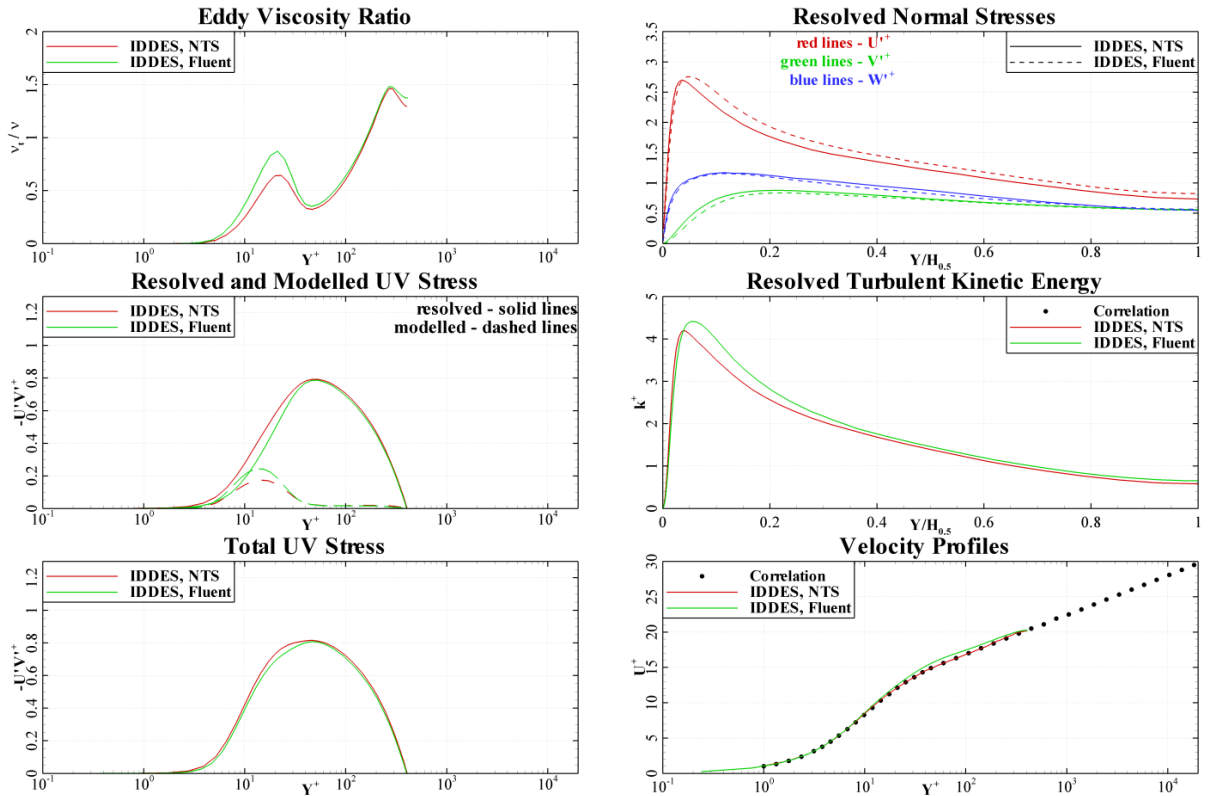
Reynolds number effect (left - $Re_\tau=395$, right - $Re_\tau=18000$)



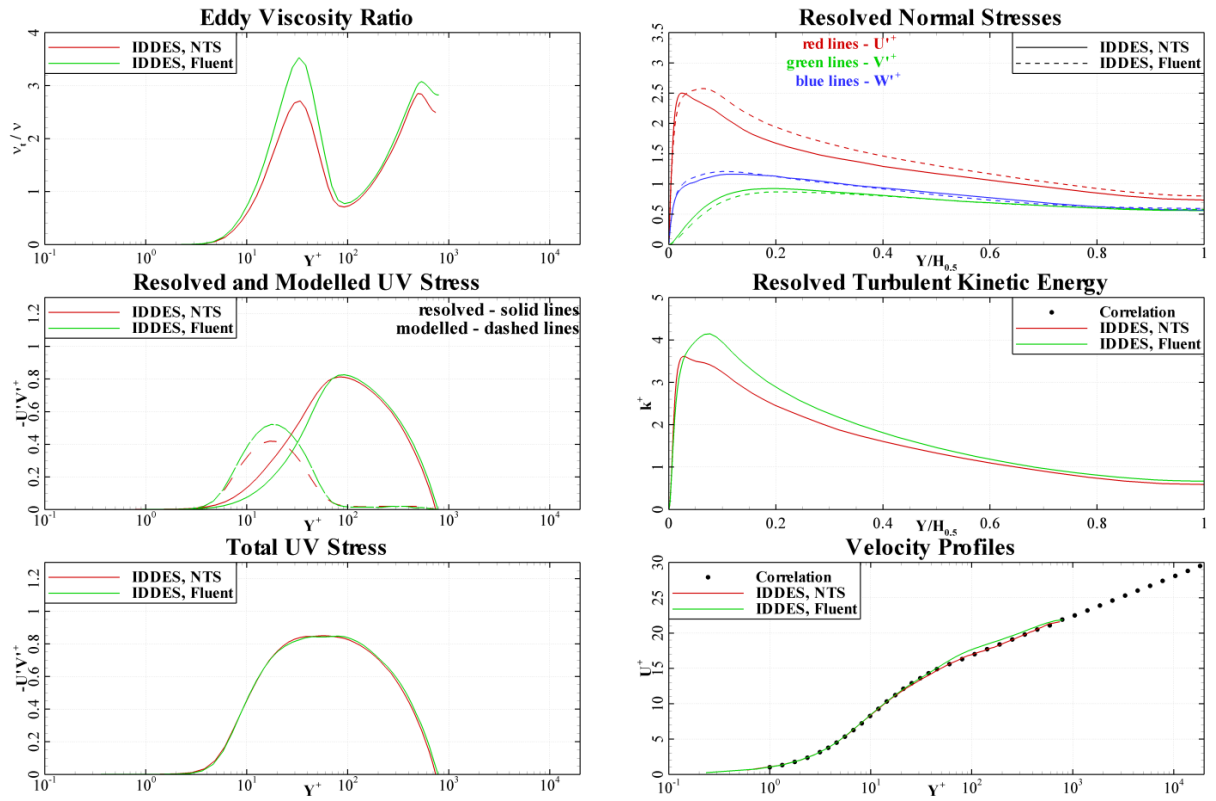
Reynolds number effect for IDDES



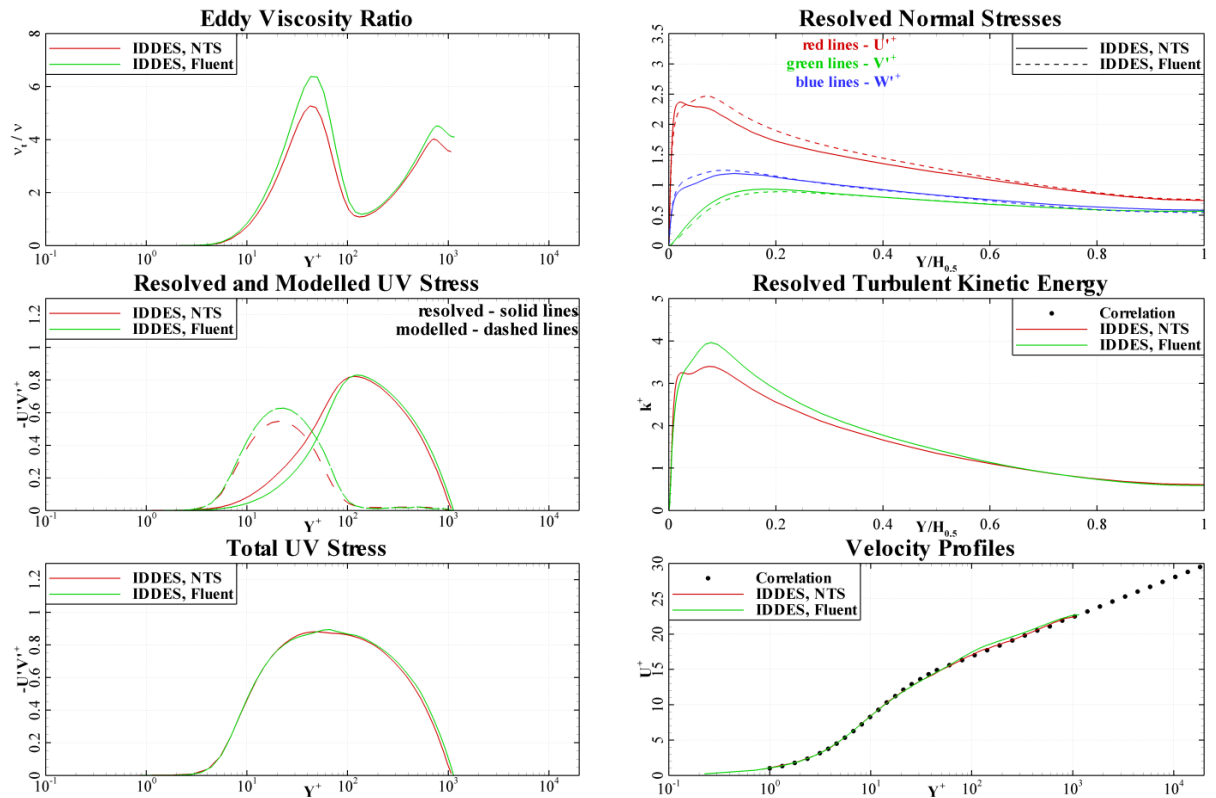
Reynolds number effect for Algebraic WMLES



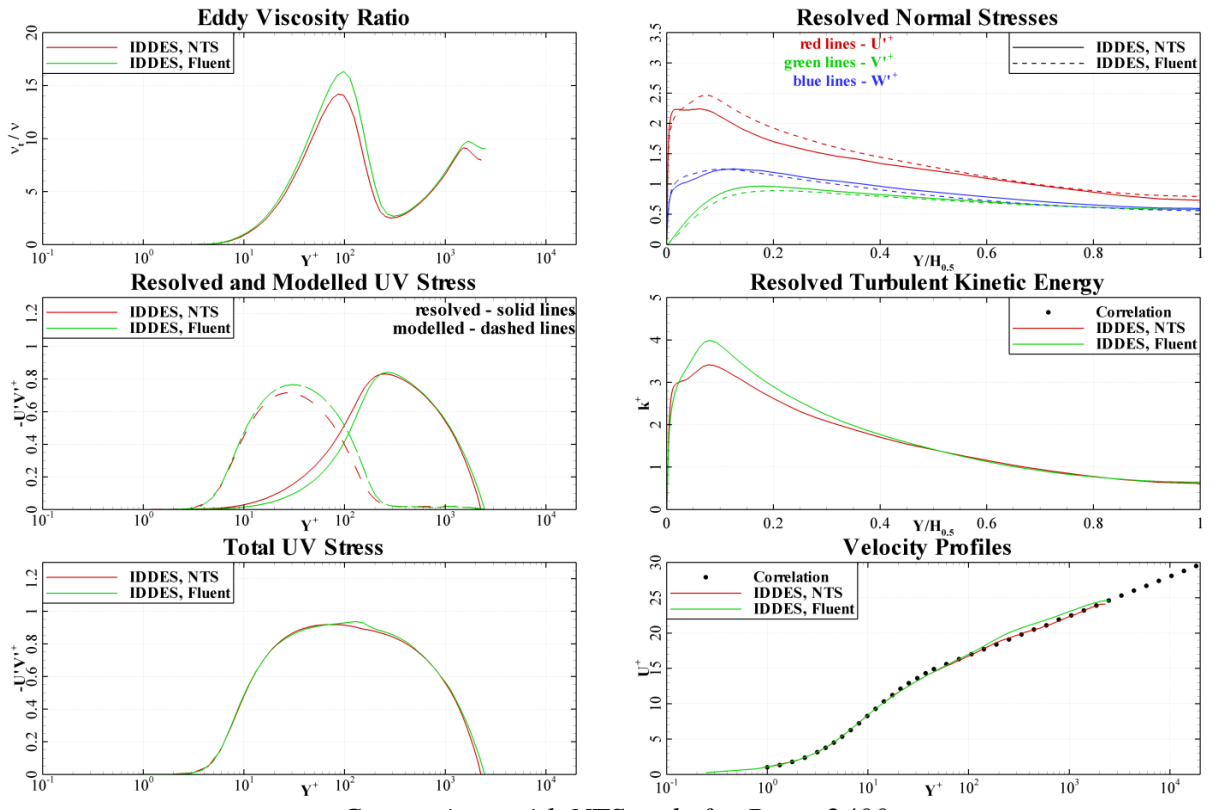
Comparison with NTS code for $Re_\tau = 395$



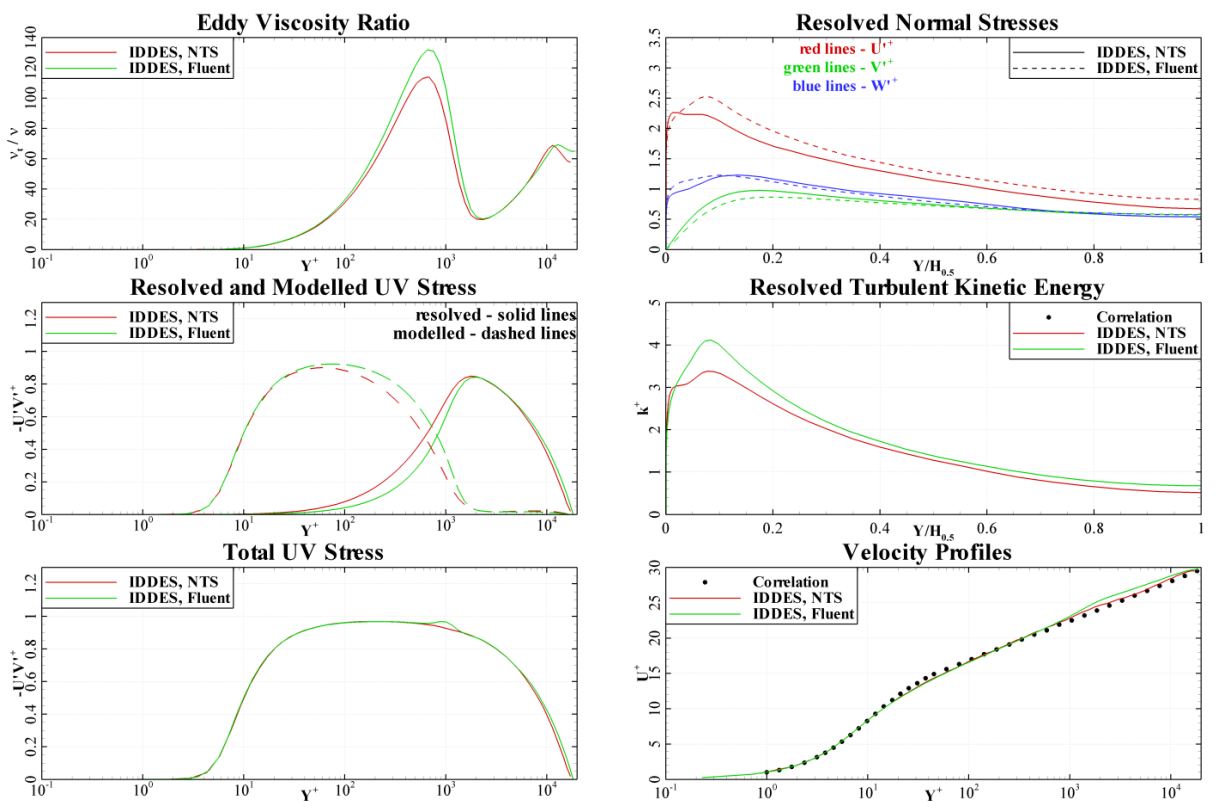
Comparison with NTS code for $Re_\tau = 760$



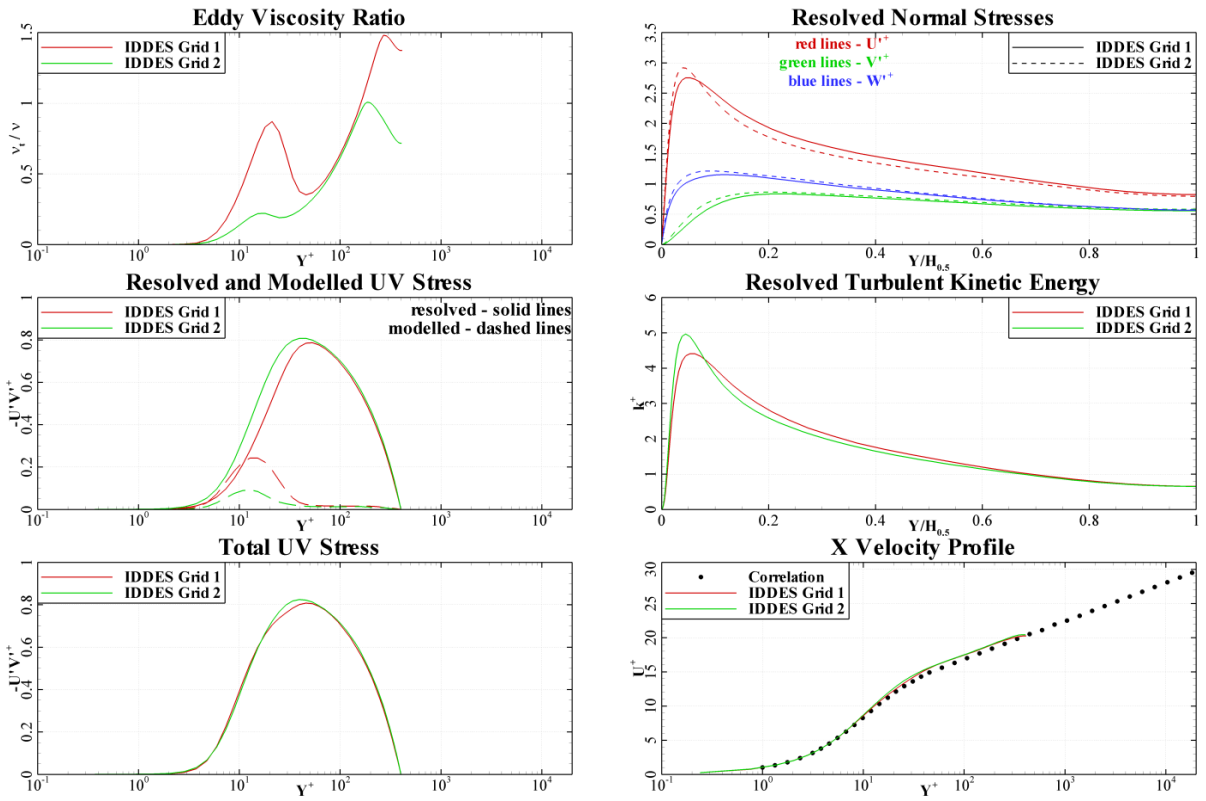
Comparison with NTS code for $Re_\tau = 1100$



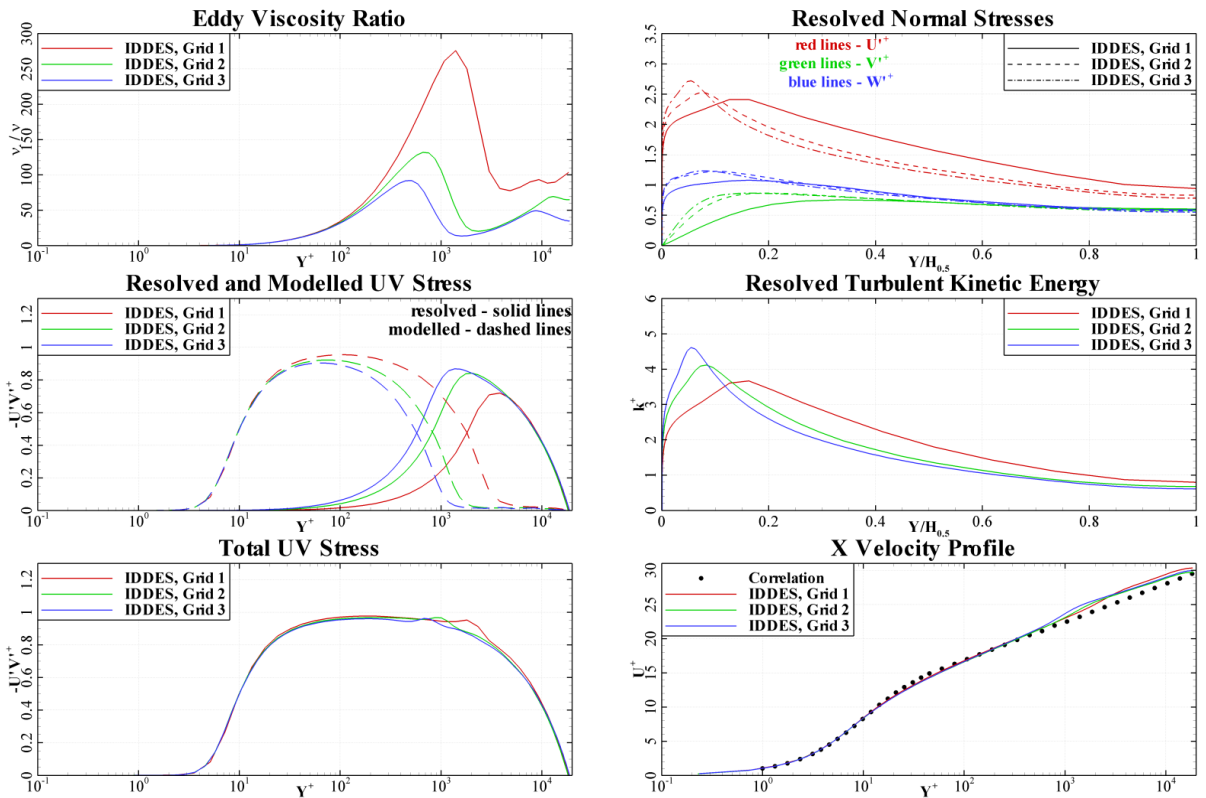
Comparison with NTS code for $Re_\tau = 2400$



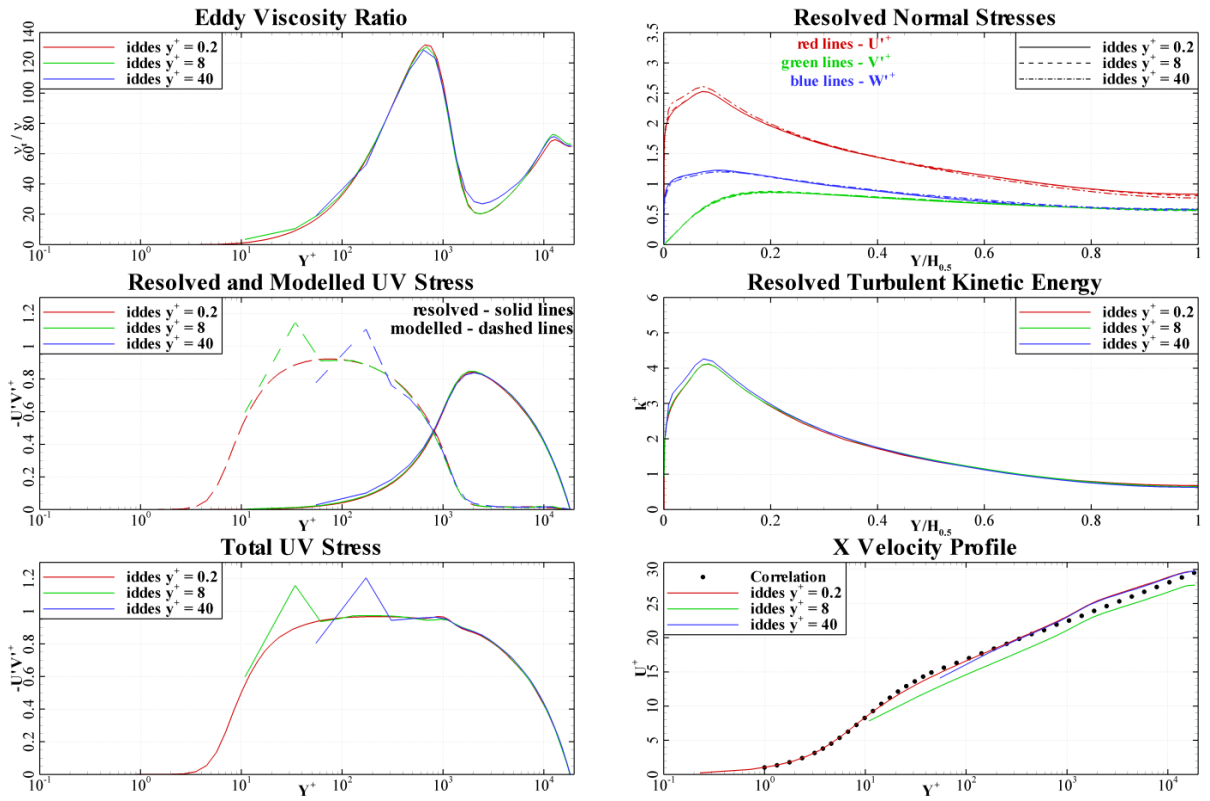
Comparison with NTS code for $Re_\tau = 18000$



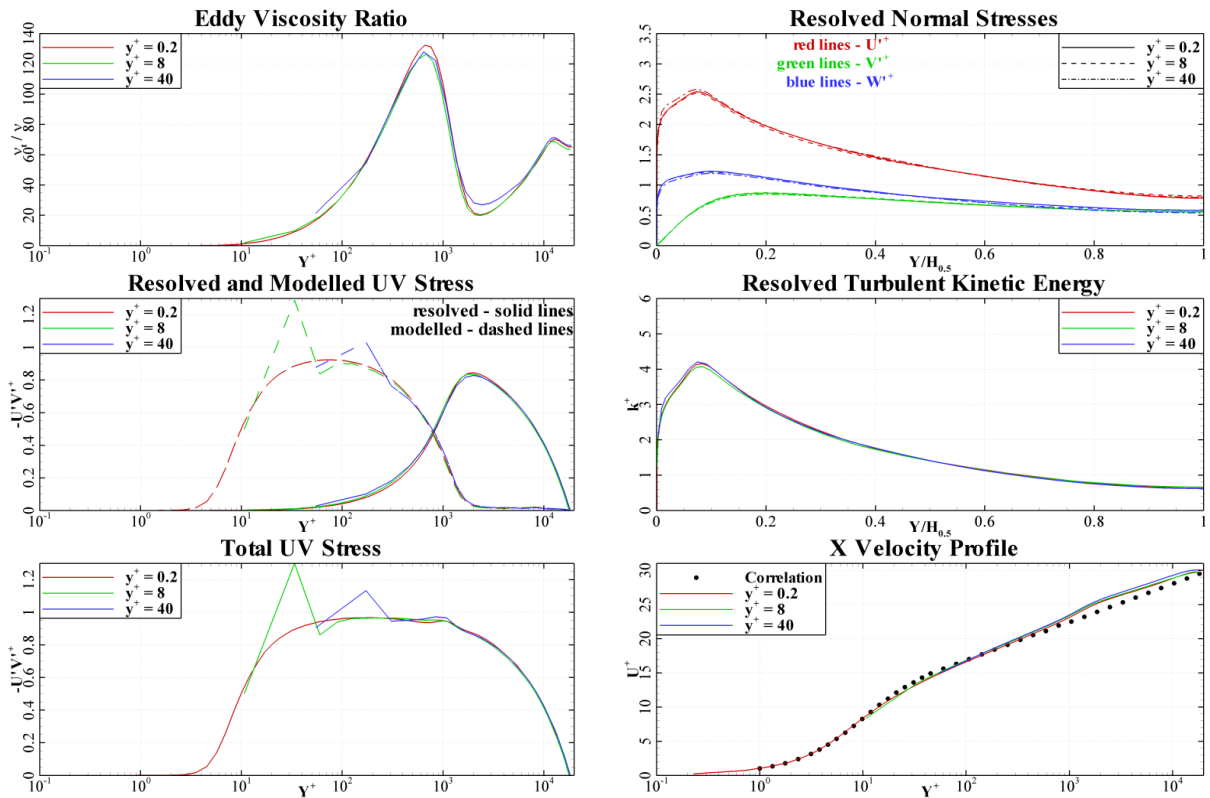
Effect of grid refinement for $Re_\tau = 395$



Effect of grid refinement for $Re_\tau = 18000$



Effect of y^+ change for $Re_\tau = 18000$ with enhanced wall functions



Effect of y^+ change for $Re_\tau = 18000$ with automatic wall functions

Summary

The SST based IDDES and Algebraic WMLES turbulence models were successfully implemented in Fluent. The behavior of the models was checked for a series of benchmark test cases.

The boundary layer protection properties for IDDES was checked and compared with DES and DDES on a Flat Plate and a NACA-4412 test case. The results of this test show that IDDES is more inclined to Grid-Induced Separation (GIS) than DES which has no boundary layer protection at all. This means that IDDES should be used very carefully in boundary layers and only suitable computational grids should be considered. Further studies which will improve the shielding of the IDDES and the DDES models are underway.

For the Backward Facing Step test case the influence of numerics and turbulence model was investigated. It was shown, that DDES with the F2 function is not appropriate for such flow, and is not recommended to use. It was also shown, that the advection scheme has a very small effect on the solution, while using of PRESTO pressure interpolation scheme leads to incorrect results, due to a delay in vortex roll-up past the step.

For the Periodic Channel test case the results were compared with the NTS in-house code. The results of both solvers agree generally well. A slightly larger velocity miss-match was observed due to Fluent's 2nd order numerics relative to the NTS code's 4th order scheme. However, this effect is small and will not impact industrial simulations noticeable. A grid refinement study was conducted for this test case. It was shown, that the results for coarse grids and large time steps are not drastically different from the results on medium and fine grids. Moreover, it was shown that the IDDES model is compatible with the automatic wall treatment and gives good results for large values of y^+ , which makes the IDDES model quite attractive for real flows.

For the Wall Boundary Layer test case an influence of numerics was investigated. It was shown that the BCD advection scheme is not appropriate for such flows likely due to increased numerical dissipation. It was also shown, that the PRESTO pressure interpolation scheme is more dissipative than all others pressure schemes and is not recommended for such SRS simulations.

References

- Coles D. and Wadcock J.** Flying-Hot-wire Study of Flow Past an NACA 4412 Airfoil at Maximum Lift [Journal] // AIAA Journal, Vol.17, No.4. - 1979. - pp. 321-329.
- Lilly D. K.** A proposed modification of the Germano subgrid-scale closure method [Journal] // Physics of Fluids 4. - 1991. - pp. 633-635.
- Mathey F. [et al.]** Specification of LES Inlet Boundary Condition Using Vortex Method [Journal] // 4th International Symposium on Turbulence, Heat and Mass Transfer, Antalya. - 2003.
- Menter F. R. and Kuntz M.** Adaptation of eddy-viscosity turbulence models to unsteady separated flow behind vehicles [Journal] // Symposium on "the aerodynamics of heavy vehicles: trucks, buses and trains." Monterey, USA, 2-6 Dec. 2002. - Berlin Heidelberg New York : Springer, 2004.
- Menter F. R., Kuntz M. and Langtry R** Ten Years of Experience with the SST Turbulence Model [Journal] // Turbulence, Heat and Mass Transfer 4. - 2003. - pp. 625-632.
- Moser R. D., Kim J. and Mansour N. N.** Direct numerical simulation of turbulent channel flow up to $Re = 590$ [Journal] // Physics of Fluids 11. - 1999. - pp. 943-945.
- Piomelly U., Moin P. and Ferziger J. H.** Model consistency in large-eddy simulation of turbulent channel flow [Journal] // Physics of Fluids 31. - 1988. - pp. 1884-1894.
- Reichardt H.** Vollständige darstellung der turbulenten geschwindigkeitsverteilung in glatten leitungen [Journal] // Zeitschrift für Angewandte Mathematik und Mechanik 31. - 1951. - pp. 208-219.
- Schoenherr K. E.** Resistance of flat surfaces moving through a fluid [Journal] // Transactions - The Society of Naval Architects and Marine Engineers 40. - 1932. - pp. 279-313.
- Shur M. L. [et al.]** A hybrid RANS-LES approach with delayed-DES and wall-modeled LES capabilities [Journal] // International Journal of Heat and Fluid Flow 29. - 2008. - pp. 1638-1649.
- Smagorinsky J.** General Circulation Experiments with the Primitive Equations [Journal] // Monthly Weather Review 91. - 1963. - pp. 99-165.
- Smirnov P. E. and Menter F. R.** Predictions of basic turbulent flows with Fluent [Journal] // Fluent Validation Report. - 2007.
- Spalart P. R. [et al.]** A new version of detached-eddy simulation, resistant to ambiguous grid densities [Book]. - [s.l.] : Theor. Comput. Fluid Dyn., 2006.
- Strelets M.** Detached Eddy Simulation of Massively Separated Flows [Journal] // AIAA Journal 2001-0879. - 2001.
- Vogel J. C. and Eaton J. K.** Combined heat transfer and fluid dynamic measurements downstream of a backward-facing step [Journal] // Journal of Heat and Mass Transfer 107. - 1985. - pp. 922-929.
- Wieghardt K. and Tillmann W.** On the turbulent friction layer for rising pressure [Journal] // NACA TM-1314. - 1951.

Numerics requirements for scale-resolved simulations on unstructured grids in ANSYS Fluent

M. S. Gritskevich, A. V. Garbaruk, and F. R. Menter

1. Introduction

Most current CFD simulations are based on the Reynolds Averaged Navier Stokes (RANS) equations. This allows the solution of complex flow problems in steady state mode with manageable computing power. However, there are numerous situations where it is not suitable to average out all turbulence content from the simulation for mainly two reasons. There are classes of flows where RANS models are not accurate enough to provide the required quality in the simulation like flows with large separation zones, largely unguided flows, and strongly swirling flows (e.g. combustion chamber flows). There also are many situations where the unsteady turbulence information is required for other models such as acoustics, vortex cavitations, FSI problems, unsteady heat loading and related fatigue. For such applications, at least a portion of the turbulence spectrum has to be resolved in at least a portion of the numerical domain. Such models are generally termed here Scale-Resolving Simulation (SRS). The accuracy of SRS is connected with two issues namely with turbulence modeling and with numerics. In current work only the later issue will be considered.

Generally speaking, different requirements for numerics are posed for RANS and SRS models. For SRS high order low dissipative schemes are required to resolve turbulent structures, while for RANS the order of scheme and its dissipative properties are not so substantial and the scheme robustness is the most desirable property. In the current work, the ANSYS Fluent CFD code is considered using different SRS approaches. This code provides a list of numerical schemes which can be used for approximating different parts of the governing equation. These schemes typically have an established history when used in combination within RANS models. At current point, there is no systematic information about the optimal application of these schemes to the SRS approach. Thus, the target of the current work is to provide comprehensive and systematic information about the applicability of the Fluent numerics for the SRS approach.

The rest of paper is organized in the following way. Firstly, in section 2 a brief description of test cases is presented. Then, in section 3 results are presented and discussed. Finally, in section 4 the conclusions are drawn and the recommendations for optimal scheme selection are provided.

Test cases description

Three test cases are considered in the framework of the current work namely the Decay of Isotropic Turbulence problem (DIT), a periodic Channel flow (Channel), and a Backward Facing Step flow (BFS). In addition to the selection of the turbulence model and the optimal numerical method, it is typically also required to provide unsteady 'LES'-inlet conditions for SRS methods. This is avoided with the selected cases, as the DIT case is set-up using periodic boundary conditions in all three space directions, the channel flow uses periodicity in the streamwise and spanwise direction, and for the BFS flow RANS inlet conditions are specified and the turbulence is generated by the flow instability past the step.

As all three flows are incompressible, the number of numerics options under consideration is significantly reduced. The solution strategies utilized in the present study are Large Eddy Simulation (LES), Monotonic Integrated LES (MILES), and Wall Modeling LES (WMLES).

Decay of Isotropic Turbulence (DIT)

The DIT problem was calculated for the conditions of the Comte-Bellot and Corrsin experiment [1] at a reference Reynolds number equal to $1.62 \cdot 10^3$, which was based on a unit reference velocity and on a unit reference length. The flow was calculated using the LES approach.

In present study the grid with 250 047 cells and 64^3 nodes was used for $2\pi \times 2\pi \times 2\pi$ computational domain. The initial energy spectrum was taken from the experiment at the first test section, up to the cut-off value of the wave number which depends on the grid size and was equal to 32 for the current grid. The non-dimensional time step was $\Delta t = 0.005$ which leads to a CFL number be less than unity in the whole computational domain. Periodic conditions were used in all three space directions. An example of turbulent structures is depicted in Fig. 1 with the use of the Q-criterion iso-surfaces colored with velocity. Henceforth the Q-criterion is calculated as $Q = |\mathbf{S}^2 - \mathbf{\Omega}^2|$, where \mathbf{S} denotes the shear strain rate and $\mathbf{\Omega}$ the vorticity.

In order to analyze the solution obtained in the framework of the problem statement outlined above and to compare it with the experimental data [1] an energy spectrum was plotted for a velocity field at two time instants obtained with the use of inversed three-dimensional Fourier transformation. For further investigation an evaluation of a resolved turbulent kinetic energy averaged over the entire domain was plotted.

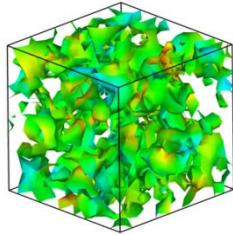


Fig. 1. Isosurface of Q-criterion colored by velocity for DIHT test case

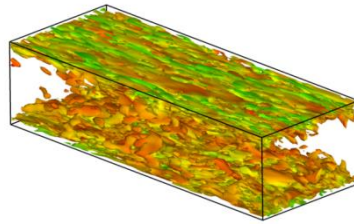


Fig. 2. Isosurface of Q-criterion colored by velocity for Periodic Channel test case

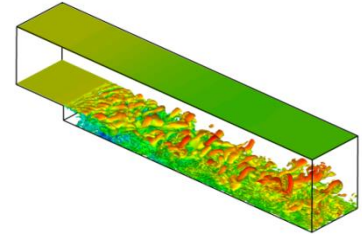


Fig. 3. Isosurface of Q-criterion colored by velocity for BFS test case

Periodic Channel (Channel)

A Channel flow was calculated for two Reynolds numbers which were equal to 395 and 18000. The Reynolds number was based on a unit friction velocity u_τ and on the unit channel height H . The low-Re flow was calculated within the MILES and the WMLES approaches, while for high-Re case only WMLES was used.

Following the calculations of Shur et. al. [2] the computational domain was $4H$ and $1.5H$ in streamwise and spanwise directions respectively. The computational grid was uniform in streamwise and spanwise direction with $\Delta x/H = 0.05$ and $\Delta z/H = 0.025$. In the wall-normal direction the grid was stretched with a factor of 1.15. It should be borne in mind that the same grid distribution in streamwise and spanwise directions was kept for both low-Re and high-Re flow. In contrast, for the wall-normal direction, the grid step in wall law coordinates was $\Delta y^+ < 1$ which allows integrating the governing equation down to the wall. A summary of major grid parameters for both considered Reynolds numbers is presented in Table 1.

Table 1. The summary of grid information for considered Reynolds number

Re_τ	Cells Number	Nodes Number	ΔX^+	ΔY^+	ΔZ^+
395	384 000	$81 \times 81 \times 61$	40.0	$0.2 \div 30$	20.0
18000	624 000	$81 \times 131 \times 61$	1800	$0.2 \div 1350$	900

Periodic conditions were applied in streamwise and spanwise spatial directions. The flow was driven with a pressure gradient $dp/dx = -2 \cdot \rho \cdot u_\tau / H$ which was taken into account in the governing equations via a source term in momentum equations.

The non-dimensional time step was $\Delta t = 0.02$ which leads to CFL number to be less than unity in the entire domain. Periodic boundary conditions were used in streamwise and spanwise direction. An example of turbulent structures is depicted in Fig. 2 with the use of Q-criterion isosurfaces colored with velocity.

In order to analyze the solutions, a velocity profile in wall law coordinates was compared with DNS data of Moser et. al. [3] for the low-Re case and with a correlation of Reichart [4] for the high-Re case. In addition, profiles of resolved turbulent kinetic energy were plotted.

Backward Facing Step (BFS)

The BFS test case was calculated for the conditions of the Vogel and Eaton experiment [5] at a reference Reynolds number equal to 28000 which was based on a unit bulk velocity and on the unit step height H . Since the flow Reynolds number is relatively high, the calculations were performed only within the WMLES approach.

Following the calculations of Shur et. al. [2], Strelets [6], and Spalart et. al. [7] a computational domain was constructed in the following way. The domain extends from $-3.8H$ to $20H$ in streamwise direction, where the coordinate origin was placed at the step location. The height of the channel upstream of the step was equal to $4H$. In spanwise direction the domain was $4H$. A computational grid had 2 251 200 cells and 2 309 715 nodes. The wall normal grid step in wall law coordinates was $\Delta y^+ < 1$ which allows integrating the governing equation down to the wall.

Periodic conditions was applied in spanwise direction. At the inlet boundary RANS profiles of velocity and turbulent quantities were used, and pressure was specified at the outlet boundary. As it was already mentioned the wall resolutions allows integrating the equations down to the wall and hence the wall treatment used on the boundary by default was insensitive. The non-dimensional time step of was $\Delta t = 0.02$ was used, which leads to CFL numbers less than unity in the entire domain. An example of turbulent structures is depicted in Fig. 3 with the use of the Q-criterion isosurfaces colored with velocity.

In order to analyze solutions obtained in the framework of the problem statement outlined above and to compare them with the experimental data of Vogel and Eaton [5] the skin friction coefficient was plotted as the most sensitive quantity.

Results and discussions

The governing equations were solved in transient mode for an incompressible fluid. A finite volume method on unstructured grids with a cell-centered data arrangement was adopted. The equations were solved using an implicit point Gauss-Seidel formulation with a Rhie-Chow flux correction [8] which is targeted to suppress unphysical pressure oscillations. An algebraic multigrid approach is implemented in ANSYS Fluent for convergence acceleration by computing corrections on a series of coarse grid levels.

As it was already mentioned above, three approaches were chosen for turbulence closure modeling, namely LES, MILES, and WMLES. For the former a Smagorinsky model with a constant equal to 0.2 was utilized. The MILES approach corresponds to the simulations with no turbulence model, which makes it possible to estimate the behavior of the numerics itself. For the WMLES simulations the Improved Delayed Detached Eddy Simulation (IDDES) model of Shur et. al. [2] was utilized.

In the Fluent code there is a wide range of numerical schemes for different parts of the governing equations which can be used in the framework of the SRS approach [9]. These schemes have different properties and their correct choice can have a significant effect not only on the algorithm performance but also on the solution accuracy. The schemes were conventionally divided into five groups namely advection interpolation schemes, pressure interpolation schemes, gradient interpolation schemes, time advancement schemes, and pressure-velocity coupling schemes. A summary for schemes falling into each group is presented in Table 2.

Table 2. The summary of numerics utilized in present work

Advection interpolation schemes	Central Difference (CD) [9] Bounded Central Difference (BCD) [9-11] Monotone Upstream-centered Schemes for Conservation Laws (MUSCL) [9,12] Quadratic Upstream Interpolation for Convective Kinematics (QUICK) [9,13] Second Order Upwind [9,14]
Time discretization schemes	First Order [9] Second Order [9]
Pressure interpolation schemes	Linear [9] Standard [8,9] Second Order [9] PREssure STaggering Option[9,15]
Gradient interpolation schemes	Cell-Centered Green-Gauss (CB) [9] Node-Based Green-Gauss (NB) [9] Cell-Centered Least Squares (LSQ) [9]
Time advancement schemes	Fractional Time Step (NITA FTS) [9,16,17] Semi-Implicit Method for Pressure Linked Equations Corrected SIMPLEC [9,18] Coupled [9]

Advection interpolation and time advancement are the most important for the SRS approach since their contribution into the scheme dissipation is much larger than for other groups. The nominal scheme order is second order for central difference schemes and goes up to third order for upwind schemes. CD is the only pure central differencing scheme, while all the rest are either pure upwind (QUICK, SOU) or blended upwind and central difference schemes (BCD, MUSCL).

Pressure interpolation and gradient interpolation schemes are less important for the SRS approach. In principle, their contribution into the scheme dissipation is not evident, albeit it should be noticed that these schemes are indirectly included into the first two groups and hence should be also investigated.

Generally speaking, the pressure-velocity coupling method should not have any contribution into the scheme dissipation, however, the robustness and the time accuracy/convergence of the computational algorithm strongly depend on this method. Herein two types of schemes are considered. The first group are so-called iterative schemes (SIMPLEC, Coupled), where for each time step inner iterations are performed to obtain the solution for the next time step. The second group are so-called non-iterative schemes (NITA FTS), where no inner iterations are required to obtain the solution for next time step. For iterative schemes, the number of iterations can have an influence on the solution since it affects the solution convergence. In the present work 5, 10, and 20 iterations per time step were considered.

For all the results obtained in further sections all the relaxation factors were set to unity to avoid uncertainties caused by convergence speed, which can cause misleading conclusions. If it is not mentioned in the text the default values for all considered test cases were CD for advection

interpolation scheme, Standard for pressure interpolation scheme, CB for gradient interpolation scheme, second order for time discretization, and NITA FTS for time advancement.

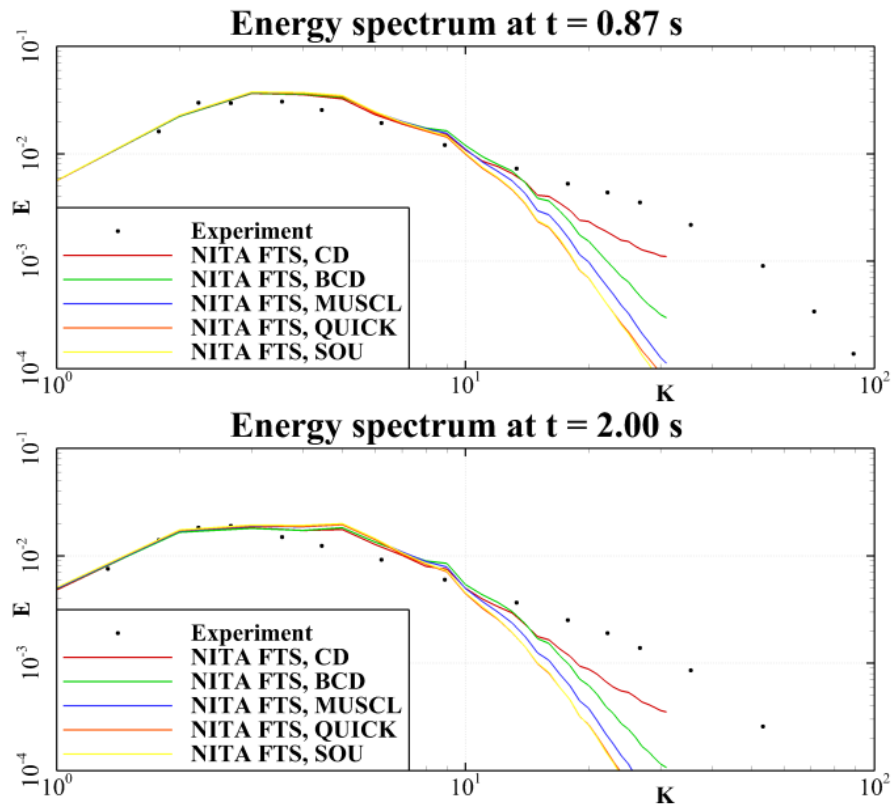


Fig. 4. Energy spectrum for the DIT test case at $t=0.87$ [s] and $t=2.00$ [s] with Smagorinsky model for different advection interpolation schemes

Advection Interpolation Schemes

Within this section an influence of advection interpolation schemes was investigated, while all the rest numerics was set by default values as it was already mentioned above.

As it was mentioned above, the calculation for the DIT problem was performed with the use of the Smagorinsky sub-grid model. The effect of scheme dissipation can be distinctly seen in the energy spectra depicted in **Ошибка! Источник ссылки не найден.** As seen, the least dissipative scheme is CD which is in better agreement with the experimental data than all others. The contribution of the scheme dissipation results in a faster drop of the energy spectrum for the smaller scales. The least dissipative from all upwind schemes is BCD, which is actually a hybrid of central difference and upwind schemes. Although it is more dissipative than the CD scheme, it can be used in situations where the energy spectrum is not the main focus of interest. As expected, the upwind/biased schemes are more dissipative than the CD/BCD schemes and dissipate the smallest scales more strongly.

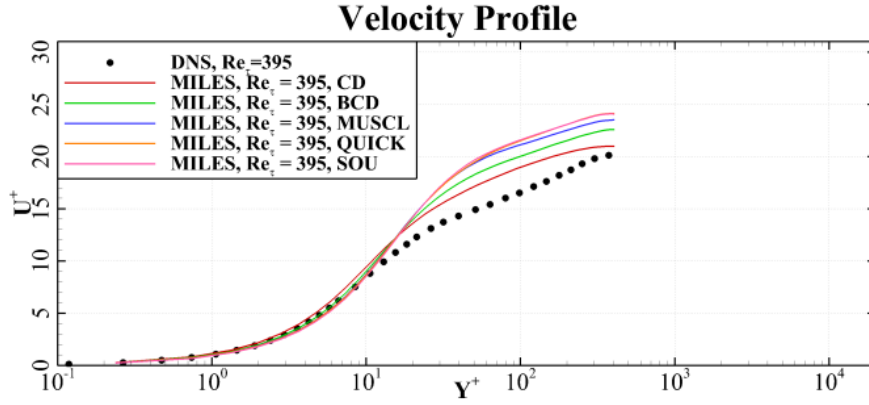


Fig. 5. Velocity profile for the channel flow at $Re_\tau=395$ with MILES for different advection interpolation schemes

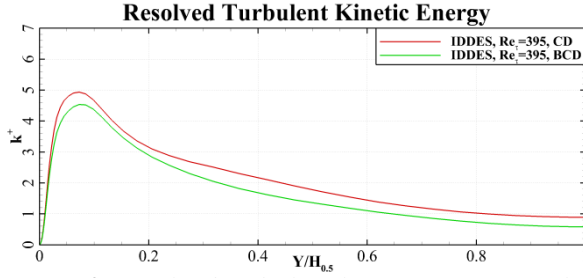


Fig. 6. Resolved turbulent kinetic energy for the channel flow at $Re_\tau=395$ with IDDES for different advection interpolation schemes

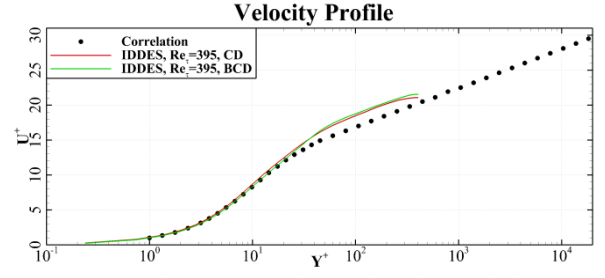


Fig. 7. Velocity profile for the channel flow at $Re_\tau=395$ with IDDES for different advection interpolation schemes

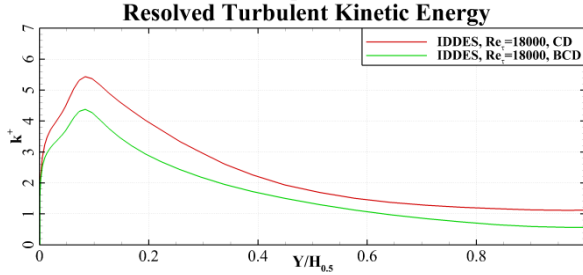


Fig. 8. Resolved turbulent kinetic energy for the channel flow at $Re_\tau=18000$ with IDDES for different advection interpolation schemes

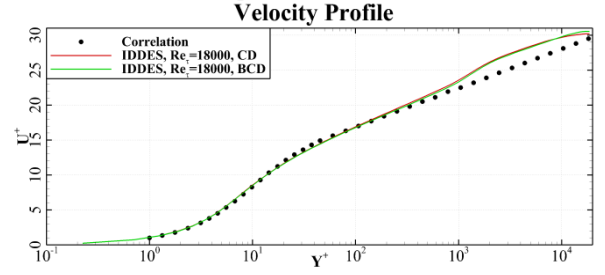


Fig. 9. Velocity profile for the channel flow at $Re_\tau=18000$ with IDDES for different advection interpolation schemes

The low-Re Periodic Channel test case was calculated with both MILES and IDDES turbulence models. For MILES all schemes from the table were considered, while for the IDDES the scope was constrained only to CD and BCD.

To estimate the effect of the scheme dissipation a velocity profile (Fig. 5) and a resolved turbulence energy profile (Fig. 6) was plotted for MILES and IDDES respectively. For the Channel test case, the effect of scheme dissipation results in so-called Log-Layer Mismatch (LLM), which can be clearly seen for MILES (Fig. 5). Thus, using the information from the velocity profile, only two schemes satisfied the requirements of the SRS approach namely CD and BCD. The performance of these two schemes was tested with the IDDES model on the Channel flow at high and low Reynolds numbers. The contribution of scheme dissipation is much smaller for IDDES than for MILES and the velocity profile do not allow to differentiate between the schemes (cf. Fig. 7 and Fig. 9). Thus, a profile of resolved turbulent kinetic energy was plotted, since this quantity is more sensitive to the scheme dissipation. As seen, BCD is slightly more dissipative than CD, however, the difference is marginal, which results in approximately identical properties of both schemes for such flow.

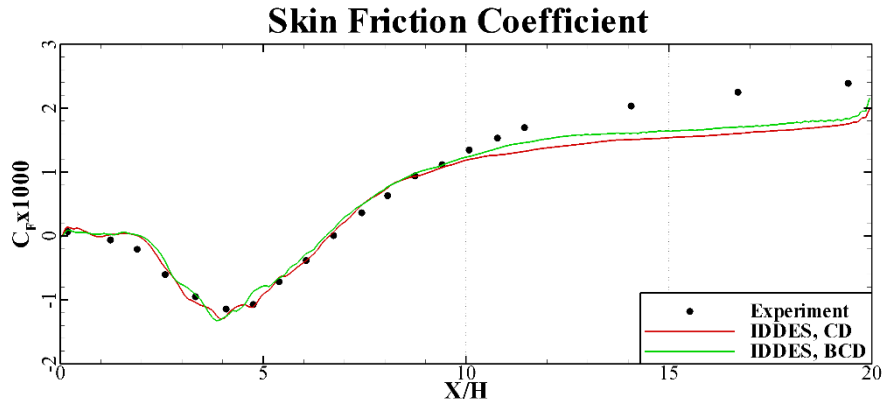


Fig. 10. Skin friction coefficient along the lower wall in the BFS flow for different advection interpolation schemes

For the higher Reynolds number, which is close to conditions in engineering applications, only the IDDES turbulence model was considered. As for the lower Reynolds number only the CD and BCD schemes were considered. As for low-Re flow the resolved turbulent kinetic energy was plotted (Fig. 8). The results shows that the difference between these scheme is larger than for the low-Re case (about 20% near the peak). However, despite this difference the scheme could be used, since typically only first order statistics is of the interest for most engineering flows.

For the BFS flow, only the IDDES turbulence modes was considered. The scope of the considered schemes was limited only to CD and BCD, since they performed well for the Channel test case. To estimate the scheme dissipation the distribution of the skin friction coefficient along the lower wall was plotted. As it was expected, no significant difference between these schemes was obtained (cf. Fig. 10).

Summing up all the results of this section, the following conclusions can be drawn. As expected, only the CD and BCD schemes are appropriate for SRS. The CD scheme is more preferable for SRS since it provides less dissipation. However, as it is reported in Mathey and Cokljat [10], in some cases CD can be unstable in the free-stream, generating unphysical wiggles which can destroy the solution. In such situations, the BCD scheme should be used instead of the CD scheme.

Time Discretization Schemes

Within this section an influence of time discretization schemes was investigated, while all the rest numerics was set by default values as it was already mentioned above.

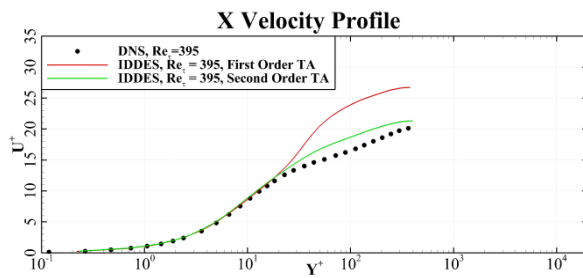


Fig. 11. Velocity profile for the channel flow at $Re_{\tau}=395$ with MILES for different time discretization schemes

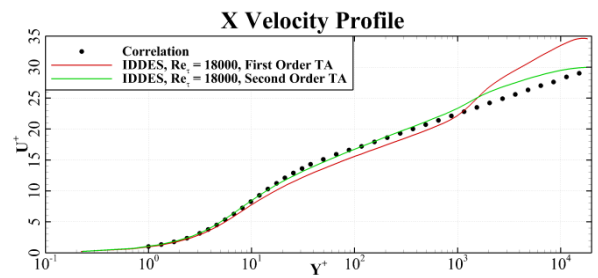


Fig. 12 Velocity profile for the channel flow at $Re_{\tau}=18000$ with MILES for different time discretization schemes

For investigating of this group of schemes, only the IDDES model was used. Two test cases were considered in this section, namely the Channel flow at both Reynolds numbers and the BFS. As seen, first order time-discretization yields a strong LLM for both Reynolds numbers. The performance of first order time-discretization schemes is very close to upwind-biased spatial discretization at least for lower Reynolds numbers (cf. Fig. 11 Fig. 12).

Surprisingly, for the BFS test case the difference between first and second order time-discretization schemes was found to be negligible. Such behavior could be explained by the strong physical instability due to the mixing layer roll-up, however, the validity of this hypothesis should be checked more properly.

Thus, summing up the results presented in this section, the order of time discretization can be very substantial for SRS in situations like in the Channel flow and if possible the second order scheme should be used.

Pressure Interpolation Schemes

Within this section an influence of advection interpolation schemes was investigated, while all the rest numerics was set by default values as it was already mentioned above.

The DIHT problem was re-calculated with the Smagorinsky model to estimate the dissipative properties of the pressure-interpolation scheme. By investigating the energy spectrum, it is found that all the schemes except PRESTO yield practically identical solutions while PRESTO gives an incorrect slope of the energy spectrum at high wave numbers (cf. Fig. 13). To understand the reason of such differences the resolved turbulent kinetic energy was plotted in Fig. 14.

As seen, using the PRESTO scheme surprisingly diminished the initial level of the resolved energy by about 12%. As a result, the subsequent solution evaluation is different from the other schemes. The reason of such difference can be seen in Fig. 15, where the energy spectrum after one time step is plotted for all the models. Therein, the PRESTO scheme is more dissipative and changes the energy spectrum even after one time step. Thus, the PRESTO scheme is suspected to be inappropriate for SRS.

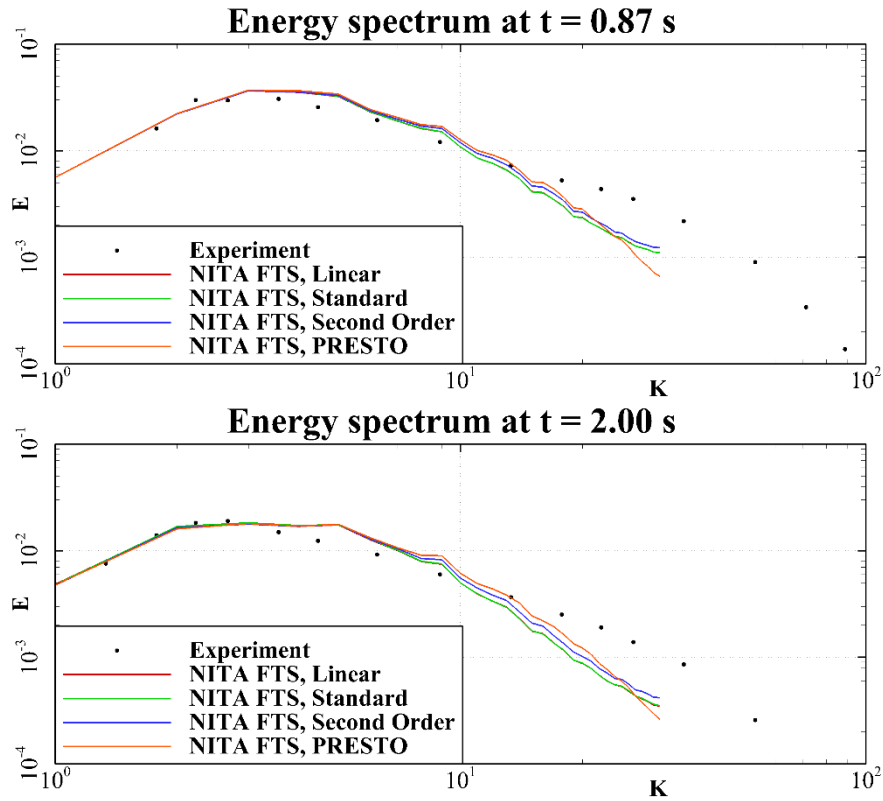


Fig. 13 Energy spectrum for the DIT test case at $t=0.87$ [s] and $t=2.00$ [s] with Smagorinsky model for different pressure interpolation schemes

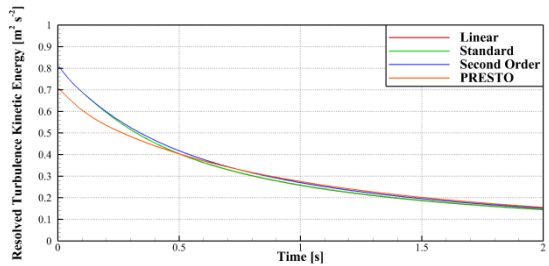


Fig. 14. Evaluation of total turbulent kinetic energy in time for the DIHT test case with Smagorinsky model for different pressure interpolation schemes

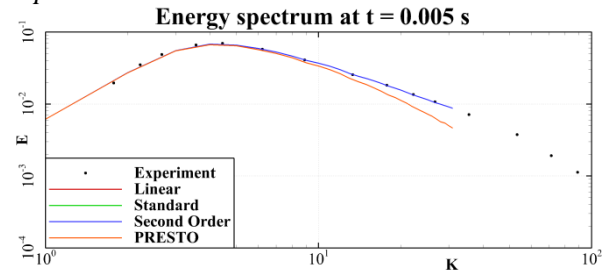


Fig. 15. Energy spectrum for the DIHT test case at $t=0.005$ [s] with Smagorinsky model for different pressure interpolation schemes

The Channel flow at low Reynolds number was calculated with both MILES and IDDES turbulence models. To estimate the effect of the scheme dissipation, a velocity profile was plotted for MILES (Fig. 16) and a resolved turbulent kinetic energy was plotted for IDDES (Fig. 17). As seen, for both models the difference between the considered schemes is not significant, however, the PRESTO scheme is slightly more dissipative than the other schemes as can be seen from the resolved turbulence kinetic energy profile (Fig. 17).

For the high Reynolds number only the IDDES model was used. As for the low-Re case, the difference between these schemes cannot be observed in the velocity profile and therefore the resolved turbulent kinetic energy was plotted (Fig. 18). The results show that there is a rather strong difference between all considered schemes. The PRESTO scheme seemed to be most dissipative since the peak in the turbulent kinetic energy is underestimated by a value of about 20%. One more observation, which is rather surprising, is that the Linear scheme is slightly less dissipative than the Standard and the Second Order schemes. This difference was not explained yet.

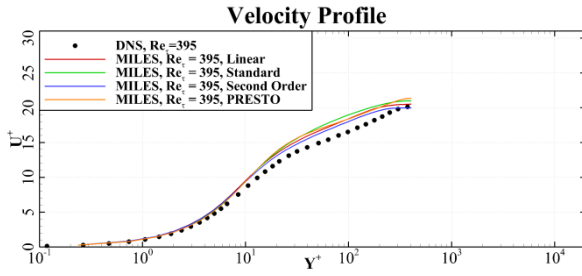


Fig. 16. Velocity profile for the Periodic Channel test case at $Re_\tau=395$ with MILES for different pressure interpolation schemes

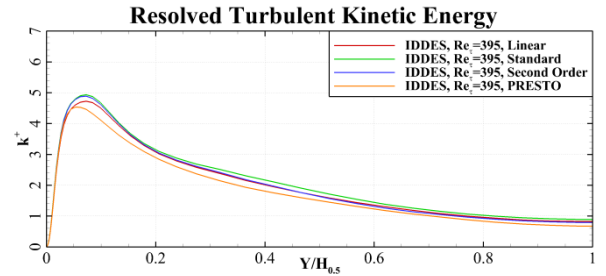


Fig. 17. Resolved turbulent kinetic energy for the Periodic Channel test case at $Re_\tau=395$ with IDDES for different pressure interpolation schemes

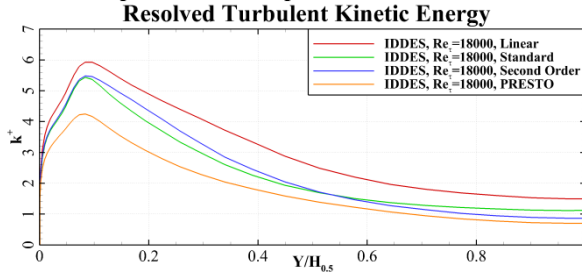


Fig. 18. Resolved turbulent kinetic energy for the Periodic Channel test case at $Re_\tau=18000$ with IDDES for different pressure interpolation schemes

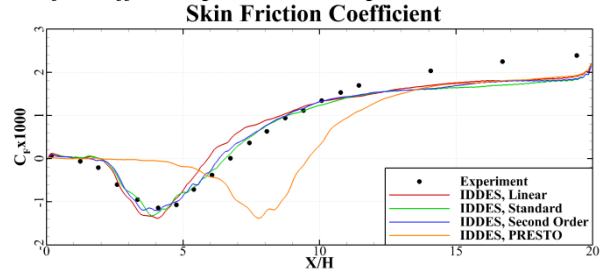


Fig. 19. Skin friction coefficient for the BFS test case with IDDES for different pressure interpolation schemes

For the BFS flow only the IDDES turbulence model was considered. To estimate the scheme dissipation, the distribution of skin friction coefficients along the lower wall was plotted. As seen, the PRESTO scheme results in an incorrect location of reattachment, while the other schemes provide approximately the correct solution.

To understand the reason of the incorrect performance of the PRESTO scheme, the vorticity contours in the XY section were plotted in Fig. 20 and Fig. 21. As seen, the mixing layer does not roll up properly, which consequently leads to incorrect mixing and a delayed reattachment processes.

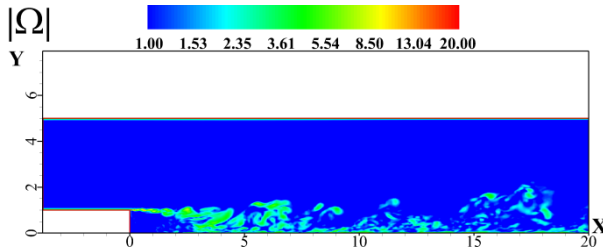


Fig. 20. Vorticity contours for the BFS test case with IDDES for the Standard schemes

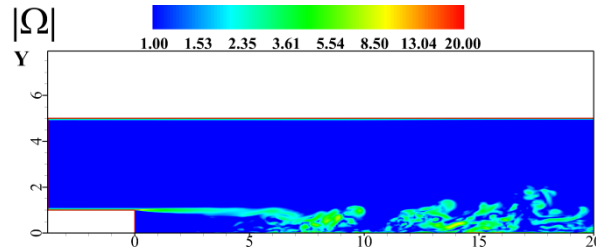


Fig. 21. Vorticity contours for the BFS test case with IDDES for the PRESTO schemes

Summing up all the results presented in the present section, the following conclusions can be drawn. Only the PRESTO scheme is inappropriate for the SRS while the rest schemes yield practically identical results and are suitable for the SRS. However, considering the scheme stability properties [9] the most preferable scheme is the Standard scheme.

Gradient Interpolation Schemes

Within this section an influence of gradient interpolation schemes was investigated, while all the rest numerics was set by default values as it was already mentioned above.

In the framework of this section, only the DIT problem with the Smagorinsky model and the Channel flow at lower Reynolds number with the MILES approach were considered. The results show that all used gradient interpolation schemes yield identical results for both test cases. However, the grids utilized in these test cases were fully orthogonal with a high quality and in such circumstances all the schemes should give the same solution. The question about dissipation properties for more complex cases is still opened.

Time Advancement Schemes

Within this section an influence of time advancement schemes was investigated, while all the rest numerics was set by default values as it was already mentioned above. As it was already mentioned above all the relaxation parameters for each time advancement scheme were set to unity.

To estimate the dissipative properties of time advancement schemes the DIT problem was calculated with the MILES model. As expected, the results for this case shows that all considered schemes result in absolutely identical energy spectra. For iterative schemes, the solution was found to be independent of the number of iterations which were equal to 5,10, and 20 in the framework of the present study.

The channel flow at low Reynolds number was calculated with both MILES and IDDES turbulence models. The results for the MILES model show that the solution is independent of the iteration number for the Coupled scheme. For the SIMPLEC scheme the solution is slightly changing with increasing iteration number. The results of the comparison of iterative and non-iterative schemes show that all the schemes yield practically identical solutions, albeit the Coupled scheme tends to be slightly more dissipative than the NITA FTS and the SIMPLEC schemes (Fig. 22). Notice that for the iterative schemes, the solutions with 20 iterations were compared. For the IDDES model the scope of computations was constrained only to the NITA FTS and the SIMPLEC schemes. It was found that both models yield practically identical results. In addition, it was found that for the SIMPLEC scheme 5 iterations is not enough to obtain a converged solution for the higher Reynolds number (Fig. 23).

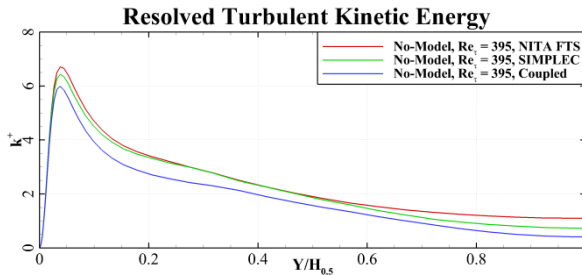


Fig. 22. Resolved turbulent kinetic energy for the Periodic Channel test case at $Re_\tau=395$ with MILES for different time advancement schemes

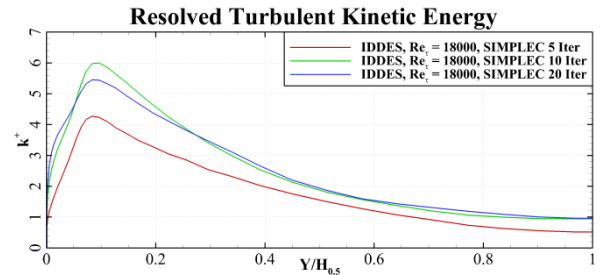


Fig. 23. Resolved turbulent kinetic energy for the Periodic Channel test case at $Re_\tau=18000$ with IDDES for SIMPLEC scheme with different iterations per time step

For the BFS flow only the IDDES model was considered. For this test case, the scope of computations was limited only to the NITA FTS and to the SIMPLEC schemes. To estimate the scheme dissipation properties the skin friction coefficient along the lower wall was plotted. It was shown, that both schemes provide practically identical results. For the SIMPLEC method 5 iterations are not enough for converged solution and at least 10 iterations are required.

Summing up all the results from the current section, the following conclusions can be made. All considered schemes provide practically identical solutions. It was found that SIMPLEC needs

at least 10 iterations for converged solutions. However, taking in account the fact that NITA FTS is the least time consuming from all considered schemes its use is quite attractive. Albeit, in some situations, especially when the grid of poor quality are used, this scheme can diverge [9] and the SIMPLEC scheme should be used.

Conclusions

A systematic study of numerics influences on the solution in ANSYS Fluent was performed. The results show, that it is possible to obtain good solutions within the SRS approach despite the fact that only low order numerics is available on unstructured grids.

Two advection interpolation schemes were considered to be appropriate for SRS, namely the CD and BCD schemes. The former scheme is preferable, however, it could provide unphysical wiggles in the free-stream and could be replaced by the BCD scheme, despite an increase in the scheme dissipative properties. Thus, a recommendation for advection scheme could be formulated in the following way. One should use the CD scheme everywhere, when it provides physical solution, and when unphysical wiggles appear the scheme should be switched to BCD.

For time discretization the most appropriate for SRS was found the second order scheme. However, in some situations like in the BFS test case using of first order scheme does not have a strong influence on the solution. However, the second order scheme does typically not cause any additional problems and is therefore recommended.

Three pressure interpolation schemes were considered to be appropriate for SRS, namely Linear, Standard, and Second Order. Using the PRESTO scheme is quite undesirable, since it is too dissipative and thus is not recommended.

All available gradient interpolation schemes provide approximately the same dissipative properties. However, considering the computational time, the CB scheme is the best choice for the SRS approach.

It was shown that it is possible to obtain good solutions within the non-iterative time advancement approach, which is very promising because of the low CPU time consumption. In case, where it is not possible to obtain a solution with the use of non-iterative schemes it is recommended to use SIMPLEC scheme with iterative time advancement, which gives practically the same results as NITA FTS.

References

- [1] G. Comte-Bellot and S. Corrsin, "Simple Eulerian time correlation of full- and narrow-band velocity signals in grid-generated 'isotropic' turbulence," *J. Fluid Mech.*, vol. 48, 1971, pp. 273-337.
- [2] M.L. Shur, P.R. Spalart, M.K. Strelets, and A.K. Travin, "A hybrid RANS-LES approach with delayed-DES and wall-modeled LES capabilities," *International Journal of Heat and Fluid Flow*, vol. 29, 2008, pp. 1638-1649.
- [3] R.D. Moser, J. Kim, and N.N. Mansour, "Direct numerical simulation of turbulent channel flow up to $Re = 590$," *Physics of Fluids*, vol. 11, 1999, p. 943-945.
- [4] H. Reichardt, "Vollständige darstellung der turbulenten geschwindigkeitsverteilung in glatten leitungen," *Zeitschrift für Angewandte Mathematik und Mechanik*, vol. 31, 1951, p. 208-219.

- [5] J.C. Vogel and J.K. Eaton, "Combined heat transfer and fluid dynamic measurements downstream of a backward-facing step," *Journal of Heat and Mass Transfer*, vol. 107, 1985, p. 922–929.
- [6] M. Strelets, "Detached Eddy Simulation of Massively Separated Flows," *AIAA Journal*, vol. 2001-0879, 2001.
- [7] P.R. Spalart, S. Deck, M.L. Shur, K.D. Squires, M.K. Strelets, and A. Travin, "A new version of detached-eddy simulation, resistant to ambiguous grid densities," *Theor. Comput. Fluid Dyn.*, 2006, pp. 181-195.
- [8] C.M. Rhie and W.L. Chow, "Numerical Study of the Turbulent Flow Past an Airfoil with Trailing Edge Separation," *AIAA Journal*, vol. 21, 1983, p. 1525–1532.
- [9] "ANSYS FLUENT 12.0 Theory Guide," 2009.
- [10] F. Mathey, D. Cokljat, J.P. Bertoglio, and E. Sergent, "Specification of LES Inlet Boundary Condition Using Vortex Method," *4th International Symposium on Turbulence, Heat and Mass Transfer, Antalya*, 2003.
- [11] B.P. Leonard, "The ULTIMATE conservative difference scheme applied to unsteady one-dimensional advection," *Comp. Methods Appl. Mech. Eng.*, vol. 88, p. 17–74.
- [12] B. Van Leer, "Toward the Ultimate Conservative Difference Scheme. IV. A Second Order Sequel to Godunov's Method," *Journal of Computational Physics*, vol. 32, 1979, p. 101–136.
- [13] B.P. Leonard and S. Mokhtari, "ULTRA-SHARP Nonoscillatory Convection Schemes for High-Speed Steady Multidimensional Flow," *NASA TM*, vol. 1-2568.
- [14] T.J. Barth and D. Jespersen, "The design and application of upwind schemes on unstructured meshes," *Technical Report AIAA*, vol. 89-0366, 1989.
- [15] S.V. Patankar, *Numerical Heat Transfer and Fluid Flow*, 1980.
- [16] J.K. Dukowicz and A.S. Dvinsky, "Approximate Factorization as a High-Order Splitting for the Implicit Incompressible Flow Equations," *Journal of Computational Physics*, vol. 102, 1992, p. 336–347.
- [17] S. Armsfield and R. Street, "The Fractional-Step Method for the Navier-Stokes Equations on Staggered Grids: Accuracy of Three Variations," *Journal of Computational Physics*, vol. 153, 1999, p. 660–665.
- [18] J.P. Vandoormaal and G.D. Raithby, "Enhancements of the SIMPLE Method for Predicting Incompressible Fluid Flows," *Numer. Heat Transfer*, vol. 7, 1984, p. 147–163.